치의학박사 학위논문

Accuracy evaluation of an augmented reality navigation system for orthognathic surgery using electromagnetic tracking

전자기적 위치추적을 이용한 악교정 수술을 위한 증강현실 내비게이션 시스템의 정확도 평가

2020 년 2 월

서울대학교 대학원

치의과학과 영상치의학 전공

김 성 하

Accuracy evaluation of an augmented reality navigation system for orthognathic surgery using electromagnetic tracking

SEONG HA KIM, D.D.S., M.S.D.

Department of Oral and Maxillofacial Radiology,

The Graduate School, Seoul National University

Objectives

An essential consideration in orthognathic surgery is the accurate positioning of the bone segment at a planned location. For this, 3D virtual skeletal model-guided surgery systems based on optical tracking were developed, and have improved surgical outcomes. However, there are also disadvantages such as the line-of-sight problem and the massive structure of the visual marker of optical tracking, and a lack of sensory feedback. In this study to overcome these issues, an augmented reality (AR) surgical navigation system based on an electromagnetic (EM) tracking was developed.

Materials and Methods

Registration is the integral part of the accuracy of the surgical navigation system. For an accurate and simple workflow, a registration body complex (the dental splint, the registration body, and the AR plane marker) and a 3D depth camera were used. The improved registration process consisted of preoperative registration and immediate intraoperative registration. The preoperative registration connected the 3D model and physical spaces of the patient using the registration body complex before the surgery. The immediate intraoperative registration connected the AR camera and the physical space automatically by the depth camera.

An invasive bone fixed reference marker is currently used in orthognathic surgery as a gold standard. In this study, a 3D-printed non-invasive reference marker was developed for a non-invasive AR surgical navigation system. The improved registration method made to maintain the accuracy since there were no manipulation errors overlapped because of the relative position of the reference marker recorded with respect to the base EM tracking tool just before the surgery.

The 3D enhanced model was produced by fusing the CT model with the high-resolution scanned maxillary dentition and applying the designated surgical landmarks, which were six anatomical structures. This 3D enhanced model improved accuracy by providing the information with quantified and visualized data of the tracking surgical landmark coordinates in real-time. And an AR information supplied by the flat-panel display was currently tracked

maxilla model of the real patient, the maxilla model of the planned position, the skull image, the occlusal plane, and the vertical axis of the skull.

The target registration error (TRE) was measured for accuracy evaluation of the improved registration method by applying an EM pointing tool to the target landmarks. The developed 3D-printed non-invasive reference marker and two types of bone fixed reference markers (reference marker in zygoma and on forehead) were used in the experiment.

For the evaluation of the intraoperative accuracy of developed AR surgical navigation and the fixability of 3D-printed non-invasive reference marker, 9 Le Fort I surgery (left lateral, right lateral, setback, advance, upward, downward, roll, pitch, yaw) was planned using a phantom which is a skull covered with soft facial tissue. The planned surgery was performed five times each, using AR surgical navigation system.

Results

The TRE of the 3D-printed non-invasive reference marker showed 0.88 ± 0.43 mm, like the bone fixed marker (0.85 ± 0.39 mm for zygoma, 0.94 ± 0.44 mm for forehead) and ANOVA tests showed no significant difference between the three reference markers. Moreover, the Le Fort I surgical results of the 3D-printed non-invasive reference marker was 0.55 ± 0.14 mm, and there was no significant difference between the three reference markers; 3D-printed non-invasive, bone fixed in zygoma, and bone-fixed reference marker on the forehead.

This result showed that the system was developed with enough surgical accuracy, and a 3D-printed non-invasive reference marker also showed fixed enough that it was applicable without the resulting difference with the bone-fixed reference marker method used currently.

Conclusion

An AR surgical navigation system for orthognathic surgery was developed, which is based on the flat-panel display, the EM tracking system, and the 3D-printed non-invasive reference marker. In conclusion, the developed system displayed acceptable accuracy and was non-invasive to the patient.

Key Words: Augmented reality, Navigation system, Orthognathic surgery, Flat-panel display, Electromagnetic tracking, 3D-printed non-invasive reference marker

Student number: 2013-30630

CONTENTS

LIST OF TABLES

LIST OF FIGURES

ABBREVIATION

AR	Augmented Reality
VR	Virtual Reality
EM	Electromagnetic
3D	Three Dimensional
2D	Two Dimensional
CT	Computed Tomography
MDCT	Multi-Detector Computed Tomography
MRI	Magnetic Resonance Imaging
PNS	Posterior Nasal Spine
ANOVA	Analysis Of Variance
HMD	Head-Mounted Display
WARM	Wearable Augmented Reality for Medicine
FRE	Fiducial Registration Error
FLE	Fiducial Localization Error
TRE	Target Registration Error
OE	Overlay Error
TE	Tool Error
NDI	Northern Digital Incorporated
AC	Alternating Current

FPS	Frame Per Second
MBS	Maxillary Bone Segment
MATLAB	Matrix Laboratory
VTK	Visualization ToolKit
SDK	Software Development Kit
NRM	3D printed skin-attached Non-invasive Reference Marker
BRM_Z	Invasive Bone-fixed Reference Marker in the Zygoma
BRM_F	Invasive Bone-fixed Reference Marker on the Forehead
RMS	Root Mean Square

INTRODUCTION

Image-guided surgery systems have been widely used in various medical disciplines.[1] The advantages of these systems are increased accuracy, reduction in surgical complications, decreased intervention time,[1,2] minimized risks, and improved surgical precision.[3] Image-guided surgery systems are mostly used (16.7% of surgeries) in neurovascular surgery[4] and are also commonly used in head and neck, general, and orthopedic surgeries.[5-7] Applying an image-guided navigation system in orthognathic surgery is beneficial for providing optimal functional and aesthetic results, patient satisfaction, and a precise translation of the treatment plan. The system also facilitates intraoperative manipulation more accurately than conventional orthognathic surgery, which uses 2D cephalometric analysis methods and plaster dental models that are mounted on an articulator.[8]

Due to the improvement in the quality of generated medical images, 3D virtual skeletal model-guided surgery systems are increasingly being used in maxillofacial surgery. These systems produce 3D models by reconstructing CT datasets and are used as preoperative planning tools for navigation systems.[9-12] The use of 3D model-guided surgery systems has made the assessment of facial deformities and the planning of reconstructive procedures easier.[13,14] A real-time navigation system for orthognathic surgery was

developed as a result of various studies, with the objective of transferring the exact course of treatment that was established in the planning stage to the actual surgical field.[15-19] The ultimate goal of this navigation system is to provide a virtual environment so that the user can feel “real” sensations. However, to overcome the lack of sensory feedback in accommodating perception views,[20] augmented reality (AR) emerged as an alternative, which worked by combining virtual objects with real-world images.

AR uses a computer-generated graphic to virtualize the patient’s images on the surgeon’s real space. In an image-guided surgery system, the development of an AR platform could result in significant improvements, provide support to surgeons, and facilitate accurate knowledge of the patient's internal anatomy and pathology.[21] AR for neurosurgery and orthopedics has already been used in minimally invasive procedures [22] and although it is being applied and developed on a large scale, it is still not widely applied in dentistry.[23] In a systematic review of the literature on AR, Farronato *et al.*[23] reported that oral and maxillofacial surgery respectively included 21 studies, which are divided into 17 for maxillo-facial, 3 for implantology, and 1 for oral surgery. This system is widely applicative and compatible with various commercial or custom equipment. Video marker-based, template-based, and infrared or electromagnetic (EM) tracking methods allow applications to track multiple objects and register the acquired surgical scene, which improves the

surgeon's perceptiveness and efficiency.[24] Consequently, if rigid structures are the focus of attention, the acquired data almost perfectly represents the intra-operative scenario, similar to performing conventional orthognathic surgery. AR systems are useful because they prevent the loss of data and time; the ease of this method was evaluated through an assessment questionnaire.[25]

The tracking system that used in currently most studied image-guided navigation system is an optical tracking system.[26-35] However, this system is not currently used well in clinical trials[30,36] due to the inherent limitations of the line-of-sight problem and a bulky structure of the visual marker.[16,17] To overcome limitations, an EM tracking system was used.[1] The small structure of the EM sensor enables its application in minimally invasive surgeries,[1,30] where it does not cause the drawbacks as mentioned above. It is small and unrestricted for ease of use in handling in the operating field, such as bone repositioning.[30] Although this is a system that covers the shortcomings of the optical tracking system, it also has disadvantages; problems with accuracy and robustness, field distortion error, need for cables to connect sensors, expensive sensors and to reuse them is complicated, technical problems of EM tracking (e.g., no patients with pacemakers, no metal near the tracking system).[30,36] Thus, continued research and development was carried out to develop an EM tracking system into a system applicable to clinicians.[37,38]

The image-guided navigation system for orthognathic surgery uses the following components: reference marker, tracking marker, and tracking system. The registration process of the navigation system is used to match the image space (obtained from the CT data of the patient) with the physical space of the actual patient. After the registration, the reference marker becomes the standard coordinate. The body of the patient and the reference marker are fixed, while the movement of the reference marker is continuously tracked during the surgery. The movement of the patient's head might be compensated because the reference marker would be able to link the CT image and the physical spaces with each other. The tracking system identifies and compares the coordinates of the reference marker and the tracking marker to visualize the relationship between their locations.

The types of reference markers used are: bone-fixed markers with screws, skin-adhesive markers, anatomic landmarks, and oral splints.[39] Orthognathic surgery requires precision, and the highly accurate bone-fixed marker is usually used as a gold standard of the reference marker, with the screws being fixed in the zygoma[30,36,40-42] and on the forehead.[8,28,32,34,35,43,44] However, these invasive bone-fixed reference markers might cause infection and scarring and may take a lot of time to attach and detach from the patient during the surgical procedure. However, non-invasive reference markers are known to have significant drawbacks, such as manipulation errors, unstable

patient fixation, and limited accuracy.[45] Nevertheless, image-guided navigation systems for orthognathic surgery are gradually developing to include non-invasive methods in the registration and tracking processes.[46]

In previous studies, an enhanced model-guided navigation system for orthognathic surgery was introduced, which used an invasive bone-fixed reference marker on the forehead based on an optical tracking.[8,32,34] In this study, an improved AR navigation system for orthognathic surgery using the EM tracking system was developed, which employed a flat-panel display, an improved registration method, and 3D-printed non-invasive reference markers. The aim of this study was to evalutae the accuracy of a developed system.

LITERATURE REVIEW

1. Augmented reality (AR) surgical navigation system

1-1. Application of AR surgical navigation system in medicine

AR is an immersive visual immersive system and is defined as “a technology that superimposes a computer-generated image on a user’s view of the real world, thus providing a composite view”.[23] One of the most promising areas for applying AR is in medical sciences.[47] During the last two decades, AR has gained immense popularity, but its use in the operating room is still under development and investigation.[48] One difference between the keywords used in medical science vs. other AR fields is the omission of the word user, which indicates that the interfaces designed for medical AR were primarily focused on achieving higher precision and not on user experience.[47] This difference is understandable as the users are highly trained professionals who need to learn to use new complex interfaces, and the precision of the interface is of utmost importance, as poor performance can be life-threatening.[47] Several research groups presented the use of augmented reality technology in many surgical fields including orthopedics,[49] neurosurgery,[50] spinal surgery,[51] minimally invasive surgery,[52,53] hepatic surgery[54] and maxillo-facial surgery[21,23] due to the possibility to meet in a more manageable and precise way the surgical procedures.[21]

1-2. AR surgical navigation system in dentistry

Several studies presented the use of AR in dentistry, including maxillofacial surgery,[33,55-60] implantology,[25,61-63] restorative dentistry,[64,65] and orthodontics.[66] Especially, maxillofacial surgery has excellent advantages in interventions carried on suitable medium-sized surgical areas. Moreover, the superposition of digital images is easier on bony structures with this technology.[67]

For maxilla repositioning (Le Fort I surgery), there are also the differences in assessment in the intraoperative position and the poor visualization of deep skeletal contours.[21] Mischkowski *et al*.[33] and Zinser *et al*.[68] presented an AR surgical method consisting of a flat-panel display and an optical tracking system, which superimposed virtual models on the image of the patient's face for computer-assisted Le Fort I surgery. Badiali *et al*.[68] showed the potential of this technique in surgical assistance by reproducing the Le Fort I surgery procedure in a phantom skull using "wearable augmented reality for medicine (WARM)", developed to use only the visible light without external infrared cameras or EM field generator. The use of AR gives the surgeon's perception of the ability to augment the virtual and real-time maxillary positions, effectively helps bone repositioning, making more comfortable and faster the performance of the surgical procedure.[24,33,68]

1-3. The tracking system of AR surgical navigation system

AR was first described in the 1960s under the title of experience theater, which involved overlaying a physical room with digitized objects.[48] Different instrument tracking systems have been proposed to enable the surgeons to infer the exact position of the instruments in the 3D world space.[48] Earlier AR systems adopted conventional sensors like optical and EM devices to establish a correspondence between different objects and to track any movements.[48] The first applications in the late 1990s utilized EM tracking systems to track movements and instruments.[69-73] The problem with this technology is that any object with magnetic properties could affect the output of the system.[48] So, in the 2000s, the trend has shifted towards optical tracking systems that are now regarded as the state-of-the-art in instrument tracks as well.[48,57,74-83] These systems are highly accurate and are available in most of the operation rooms today because of their optimum performance.[48,83]

1-4. Visualization device of AR surgical navigation system

It is imperative to present instrument information using a user-friendly interface along with surgical planning and navigation data.[48] AR systems can be classified into two types, based on the level of the sensation of being inside a particular environment: immersive (direct) and semi-immersive (indirect).[48]

Immersive AR refers to the systems in which the user visualizes the real environment directly, and additional information is projected over the environment.[48] Whereas semi-immersive AR refers to the systems in which the user is partially disconnected from reality and cannot receive the proprioception information directly on his body.[48] In the operating room, AR can theoretically be delivered through smart glasses or headset, half-silvered mirror, flat-panel display monitor, loud-speakers, gloves, joysticks, or co-manipulated robots, and so on.

Numerous options have been explored for visualization of the AR output, such as traditional displays, wearable technology, see-through, and projection devices; however, no standard practice has been established for clinical practice.[48] The most popular display in cranial base AR systems is the traditional surgical monitor.[75,77,80,81,84-86] The conventional approach is to present the pointing tool on the three orthogonal planes of the preoperative data.[69,72,74,77,87] However, it is difficult to manipulate the surgical instruments ergonomically for the surgeon. Innovations that display the instrument information on 3D display screens or augmented/virtual 3D environments will be highly beneficial and ease the task of the surgeon.[48] The disadvantage of using traditional surgical monitors is that they do not provide any depth cue.[48] Alternatively, the instruments can be highlighted in different colors based on the distance between the planned position and the target structures.[69,71,77,80] The

surgeons have to rely on color to infer the distance between the pointing tooltip and the target structure. Text-based information is often added to the display to facilitate the surgeons.[88]

As a substitute to conventional traditional surgical monitor, visualization devices of AR surgical navigation system may be classified into three categories:

(a) See-through projection systems using HMD (using smart glasses or a headset).[25,56,63,68,72,73,89,90]

(b) Projection systems using a half-silvered mirror which guided surgery using a semi-transparent screen.[59,91]

(c) Systems to project digital data onto a flat-panel monitor which guided surgery based on the transfer of digital data to a monitor display.[33,64,65,92,93]

HMD is a device worn on the head that has a small display in front of the eyes. Some HMDs also have the ability to project images, allowing the user to see through them. HMDs used in surgery can superimpose computer-generated virtual objects over real-time video.[48] Most studies have found that wearable HMDs for surgery usually results in improved ergonomics compared to traditional procedures in which the surgeon is required to turn his or her head repeatedly to shift visual focus between the surgical field and the imaging monitor.[92] HMDs allow surgeons to concentrate on the task at hand without having to turn their heads away from the surgical field constantly.[94,95] In AR

systems, a half-silvered mirror projects a display similar to HMD, but it is not a wearable device. A flat-panel monitor (tablet) have also been utilized in different applications to display hidden structures that do not require large incisions in craniomaxillofacial procedures.[33]

The drawbacks of these visualization devices of the AR surgical navigation system are collected in Table 1. Inattentional blindness refers to the failure of noticing a fully-visible, but unexpected, object because attention was engaged on another task, event, or object.[96] The HMDs provide ergonomic benefits, such as direct visualization, as compared to visualization on surgical monitors; they have been shown to increase inattentional blindness, especially when an unexpected situation arises because they have the small size of the screen.[81] One of the major problems that arise in many studies involves eye strain (asthenopia) associated with concentrating on a screen for prolonged periods.[97] As with viewing of any sort of imaging monitor, prolonged usage can lead to visual discomfort (ocular fatigue, discomfort, lacrimation, and headaches arising from the use of eyes).[98] This discomfort is a problem with not only wearable devices but also imaging devices in general, including medical imaging monitors that are traditionally used.[99,100] If the operative field and the virtual objects are not projected on the same plane, eyes fail to accommodate such out-of-focus images, the focus problem is due to this reason.[79] Latency is a lag in the display of the real and virtual information

cannot be tolerated in a surgical environment.[79] Due to the low rendering speed of the system, displaying enriched information is not possible.[48] Battery power is another drawback that must be addressed because of long operative times inherent to certain surgeries.[98] For example, when used for streaming or broadcasting, the Google Glass battery life can be as little as 30–40 minutes.[95,101] The heavy and bulky devices are the reason that many surgeons are not comfortable wearing HMDs.[79]

Table 1. The drawbacks of the visualization devices of the AR surgical navigation system.

Drawback	Head-mounted display	Half-silvered mirror	Flat-panel monitor
Inattentional blindness	O		
Eye strain (asthenopia)	O	O	O
Focus	O	O	
Latency	O	O	
Battery power	O	O	
Heavy and bulky devices	O		

The HMDs, in general, have not been a popular choice among practitioners in clinical practice due to the many drawbacks. Although the HMD based system is the most classical use of AR in other various fields, flat-panel monitor based systems are considered the majority in dentistry.[23] However, in

AR surgical navigation systems, the best option indeed is one where the virtual information is directly projected on the surgical site as it allows for direct visualization and improved ergonomics.[48,102] And it is important to understand that virtual information reduces the visibility of the surgical site and consequently as it may reduce on-site visibility by obstructing important structures or lead to visual discomfort, displaying virtual objects during the entire surgical duration does not seem to be ergonomic.[48] The efficiency of the system may improve if virtual structures are overlaid only when they are required and not throughout the procedure.[77,80,103]

1-5. Accuracy evaluation of AR surgical navigation system in maxillofacial surgery

Different factors contribute to the final accuracy and evaluation of the surgical navigation system:[48]

(a) Fiducial registration error (FRE) depicts the difference between positions of fiducial points (often used for registration) in the preoperative images and their corresponding points on the patient coordinate system.

(b) Fiducial localization error (FLE) is the distance between measured and actual positions of the fiducial points caused by discrepancies in the image and patient coordinate systems.

(c) Target registration error (TRE) defines the intraoperative distance between actual positions of target localization and their corresponding positions in the patient coordinate system. It is often regarded as the final accuracy of the system.

(d) Overlay error (OE) is similar to TRE but defines the difference in an overlap of projected virtual information and their corresponding structures in physical space. It is usually measured from the boundary points of the projections.

(e) Tool error (TE) is the error in the determination of the position and orientation of surgical instruments being used to carry out the procedure.

All of the above parameters are essential characteristics of an AR system and necessary for evaluation. However, it is recommended that TRE should always be quoted as it encompasses different types of error into one and provides an excellent intuition to the expected overall accuracy.[48] TRE is defined as the displacement of a specially chosen point (for example, an anatomical point, not the fiducial used for registration) in virtual space compared to physical space.[104] AR surgical navigation systems that are commercially available have achieved target accuracies of around 1.5-2 mm.[48] However, recently researchers have realized that attaining surgical errors below 1 mm is infeasible due to the physical limitations of the anatomy and system. Thus, maximum errors of 1.5-2 mm have been regarded as plausible.[105,106]

Most of the maximum TREs observed were less than 2 mm (Table 2).[102] These values are not different from those typically observed in navigation for maxillofacial surgery in humans.[107] It is essential to mention that in a surgical application, results may differ significantly from those in laboratory conditions.[48] It can be inferred that the accuracy almost drops by 45% when a shift is made from the laboratory to the operating room.[80,86,88]

Table 2. The TRE values of AR surgical navigation system in maxillofacial surgery in previous studies (unit: mm).

Study	TRE	Max	Min
Wang *et al*. 2019[108]	0.42	0.71	0.24
Wang *et al*. 2017[57]	0.82	1.65	0.67
Zhu *et al*. 2017[109]	0.95	2.00	0.55
Zhu *et al*. 2016[110]	2.17	3.30	1.26
Lin *et al*. 2016[111]	0.95	1.26	0.67
Suenaga *et al*. 2015[112]	0.57	0.71	0.25
Lin *et al*. 2015[113]	0.73	1.47	0.04
Wang *et al*. 2014[114]	-	1.03	0.71
Suenaga *et al*. 2013[59]	0.77	1.34	0.45
Mischkowski *et al*. 2006[115]	0.84	1.67	0.43
Total		3.30	0.24

2. Electromagnetic (EM) tracking system

The tracking system initially used in the navigation system of maxillofacial surgery was an optical.[8,26-35,116,117] The optical tracking navigation system has achieved widespread acceptance, and though manufacturers claimed reliability and accuracy.[118] Basically, the optical tracking navigation system has an optical camera and visual marker, so is the structure of the camera tracks the marker. If interruption exists between camera and marker, it cannot be tracked with the following. In this reason, this system had drawbacks; the line-of-sight problem and a bulky visual marker.[16,17,119-122] Therefore, the optical tracking system is not widely used.[36]

In the 1970s, the EM tracking navigation system was developed by an idea of sensor localization utilizing magnetic positioning.[123] In general, the EM tracking navigation system is composed of a magnetic sensor, field generator, and tracking system. The magnetic sensor is a thin pin-type sensor that is 0.5 mm to 1 mm long and has an "implantable" structure anywhere. The small structure of the magnetic sensor enables its application in minimally invasive surgeries in the area of percutaneous factors, catheter applications, and endoscopic applications.[1,30] The field generator type is divided into standard, flat, mobile, and long-range, which is smaller than the optical tracking navigation system but provides sufficient working volume to perform orthognathic surgery.[30] The commercial systems currently most used are

Aurora of Northern Digital Inc. (NDI, Waterloo, Ontario, Canada), EM tracking system based on a dc-driven magnetic field of Ascension Technology (Burlington, VT, USA), ac-driven EM tracking devices of Polhemus (Colchester, VT, USA), and so on.[30] As such, the EM tracking navigation system uses a small magnetic sensor and a magnetic field, so it does not cause the drawbacks mentioned above. In other words, the electronic tracking navigation system eliminates shortcomings in the optical tracking navigation system, and it might hold the sensor in the desired position during image-guided orthognathic surgery.

EM tracking navigation system has a few drawbacks. The most representative one is field distributed error. This error is the phenomenon where the magnetic fields are interfered by ferromagnetic materials and other fields in the surrounding area, and this is an error caused by the development of the magnetic field detachment by other ferromagnetic objects, such as medical diagnostic devices like CT or MRI scanners, or various metrological objects used during surgery.[1,30,36,124,125] This error results in a problem in the accuracy and robustness of the EM tracking navigation system. Another drawback is that instead of being free from line-of-sight problems, the EM sensor is connected by a cable to the tracking system. For this reason, there is an increase in entrapment and surgical time and efficiencies in the process, such as osteotomies and bone removals when used in orthognathic surgery, and in

severe cases, it is uncomfortable to break down with iatrogenic factors.[1,41,44] Since the EM tracking system is a method that offers no line-of-sight problem,[119] research on this topic has continued for many years and has resulted in the development of technology and improvements in the software design (e.g., reduction of the sensor size, increased accuracy).[37,38,40] Thus, EM tracking has become suitable for use in the navigation systems of orthognathic surgery.[40]

On the accuracy side, NDI Aurora and Polhemus Fasttrack have much lower distribution errors.[126,127] Studies compared to the optical tracking system showed similar accuracy with EM tracking system.[128-131] In many papers, EM system accuracy is reported to be less than 1 mm,[1,30,58,132,133] resistance deviation, measured by setting up phantom skull in operating room condition, also showed high accuracy and perfected stand results similar to that of the optical tracking system.[30,43] Berger *et al*. concluded that even when applying the EM tracking system to Le Fort I surgery conducted using a phantom skull, the results were sufficiently successful.[36] On the field distortion error side, the NDI Aurora was able to track closer to all the test distorter types.[129] Small metallic objects of the same degree as the dental bracket or stainless steel wire in the application of orthognathic surgery do not affect the accuracy of NDI.[30,43,134] Large metallic objects, such as the langenbeck retractor, may affect accuracy, however in actual clinical applications, the tracking system able to be performed with removal in advance, and in case of this, the EM error detection

option may provide automatic intraoperative real-time warning, which helps to detect severe interference in advance to compensate for the error.[1,134-136] As such, the current EM tracking system has developed into a system that is very suitable for use in orthognathic surgery.[41,122] And most of the surgeons were convinced that the system allowed increased accuracy in maxillary positioning.[43]

The EM tracking navigation system, which shows the acceptable accuracy, is being used and developed in two significant ways within the orthognathic surgery; the system used for mandibular proximal segment repositioning to reduce positional displacements of the condyle through orthognathic surgery,[41,42,44] and the system that increases accuracy of maxillary or mandibular position by applying it directly to orthognathic surgery.[36,43,136] In the previous study, an EM system based surgical method that provided real-time 3D enhanced model-guide was developed, and the 3D condyle-fossa positional relationship was made more accurate.[44]

3. Non-invasive reference marker

The development of a non-invasive surgical method is the aim of computer-aided surgery.[46] In the image-guided navigation system, there are several markers must be very rigidly fixed to the patient for improved accuracies, such as the fiducial marker used during registration, reference marker to achieve the rigid body with the patient during navigation, and tracking marker. Several methods have been developed, including skin-adhesive markers, anatomic landmarks, oral splints, and laser scans to non-invasively apply this system,[39] however, the use of these methods was found to affect the TRE negatively.[137-141] In particular, since the early 2000s, many studies have been conducted to measure and compare the invasive bone fixed markers and TREs by applying skin-adhesive markers as a reference marker, but as a result, the skin-adhesive method shows much larger TRE values than the invasive bone-fixed method and is reported to be unsuitable for clinical applications.[45,137,140,142-146] The reasons for such low accuracy were user manipulation errors, swelling due to patient sedation, unstable patient fixation, suboptimal registration of the fiducial marker configuration, and tracked tool calibration errors.[147-151] Thus, the reference marker of the surgical navigation system that employs the bone-fixed screw is still used as the gold standard,[143-146] and the overall negative positions of the skin-adhesive marker is expressed.[36]

4. 3D printing in dentistry

Due to the steady development of the process and material of 3D printing technology, many 3D-printed models are applied to the image-guided navigation system. It is incorporated into a variety of medical fields (traumatology, orthopedics, neurosurgery, implant dentistry, plastic surgeries, craniomaxillofacial surgeries) and is designed to increase the precision of surgery.[152] 3D-printed model is made of phantoms or models and used for treatment planning, simulation (rehearsal) of surgery,[153-155] and make implant, and bone graft which used in reconstruction and used in combination with navigation or radiation,[3,156-158] and the positioning guides are manufactured and used for surgery,[159-162] also used for doctor-patient communication. As such, 3D-printed patient-specific models can be used in a variety of ways, including treatment planning, intraoperative procedure, postoperative evaluation, which is a benefit of optimal functional and aesthetic results, patient satisfaction, and precise translation of the treatment plan.[163] Like this medical trend, 3D printer is used in orthognathic surgery to manufacturing occlusal splints,[164-167] osteotomy/cutting guides and repositioning guides,[33,113,168-170] spacers,[171] fixation plates/implants,[172-175] and 3D-printed models.[176-179]

MATERIALS AND METHODS

1. Acquisition of CT data and 3D dentition scan, and experimental setup

A phantom, which is a skull covered with soft facial tissue (Sawbones, Pacific Research Laboratories Inc., Vashon, WA, USA), was used to evaluate the developed AR surgical navigation system for orthognathic surgery (Fig. 1). The CT data of the phantom was obtained with 0.75 mm slice thickness under 120 kVp, 80 mAs using MDCT (SOMATOM Sensation 10, Siemens, Munich, Germany). The phantom was occluded with a dental splint attached to a registration body before CT imaging. The dental splint was manufactured using an orthodontic self-curing acrylic resin (Ortho-Jet, Lang Dental Manufacturing Co, Wheeling, IL). The registration body with fiducial holes of ceramic spheres (1 mm in diameter) was attached to the splint with a Lego block (LEGO Group, Billund, Denmark) for registration. The surface models of the skull phantom were generated by applying the marching cube algorithm to the CT image data.

The maxillary plaster casts of the phantom were scanned optically using a scanner (Maestro 3D, Maestro, Pisa, Italy) to obtain a high-resolution model of the maxillary dentition.[180-182] The scanned dentition models were fused with the CT surface model by registration using an ICP algorithm.[44]

Furthermore, the virtual skeletal models were produced by cutting according to the plane used in the actual surgery. The 3D enhanced model was generated by added six surgical landmarks (upper right first molar, upper right canine, upper right incisors, upper left incisors, upper left canine, upper left first molar) to the virtual skeletal model. The surgical landmarks are an anatomical structure (tooth) that can be checked directly during surgery, and it is a significant indicator that constructs an occlusal plane when solving facial asymmetries.

The skull phantom was connected to an operating table by using a ball-socket joint for simulating free movements of the phantom's head during surgery (Fig. 1). The flat-panel display monitor (QCT130, G One Inc., Seoul, Korea) equipped with a depth camera (Realsense, Intel, California, USA) at its back was positioned between the surgeon and the phantom by using a supporting arm (Fig. 1). The camera could measure 3D coordinates of objects with a resolution of 1280x720 pixels at a rate of 30 fps. The display provided the surgeon with visualized and quantitative information of the AR simultaneously during surgery. An EM tracking system (Aurora, Northern Digital Inc., Waterloo, Canada) and miniaturized EM tools (sensor) were used to track the 3D position of the maxillary bone segment (MBS) in the physical space (Fig. 1).

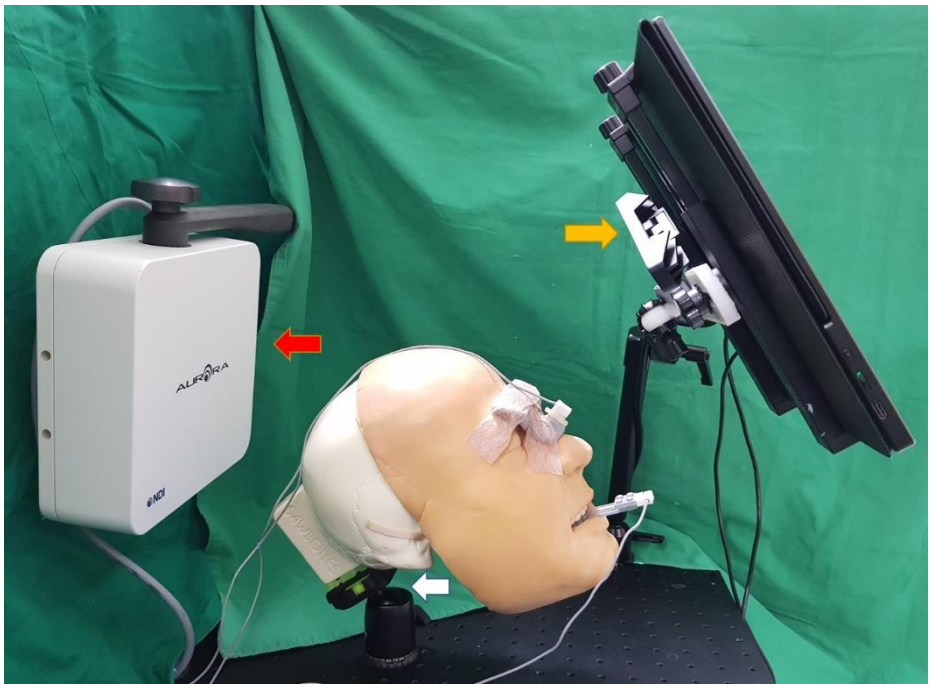

Figure 1. The operating table was designed to connect the ball socket joint (by the white arrow) between the phantom and the operating table, so that the head might move freely like a real patient during actual surgery. The AR flat-panel display monitor equipped with a depth camera (by the yellow arrow) was positioned between the operator and the phantom by using a supporting arm. The EM tracking system (by the red arrow) was installed about 10 cm apart at the bedside of the phantom.

2. 3D-printed non-invasive reference marker and EM tracking tool of separable frame

The 3D-printed non-invasive reference marker base for installing the EM tracking tool (sensor) was fabricated by 3D printing. The position of the reference marker base was selected flexural and rigid support, located beside the taboo region,[140] such as the eyelid or tip of the nose. From the metrological study of the face (Anthropometry),[183-187] a T-shaped base was designed containing part of the eyebrow, glabella, and nasal bone, which showed no interference with nasotracheal intubation and the minimal effect by the head movement during surgery, where the facial skin was thin and less affected by swelling (Fig. 2). A patient-specific reference marker base was made to combine this T-shaped base with the CT image of the patient and created using the stereolithography 3D printer (Fabpro 1000, South Carolina, USA) at 65-μm resolution. This 3D-printed non-invasive reference marker was rigidly attached to the patient's skin by using a surgical tape (3M Micropore Surgical Tape, 3M, Minnesota, USA) non-invasively while the bone-fixed reference marker was fixed on the patient's skull with a bone screw invasively.

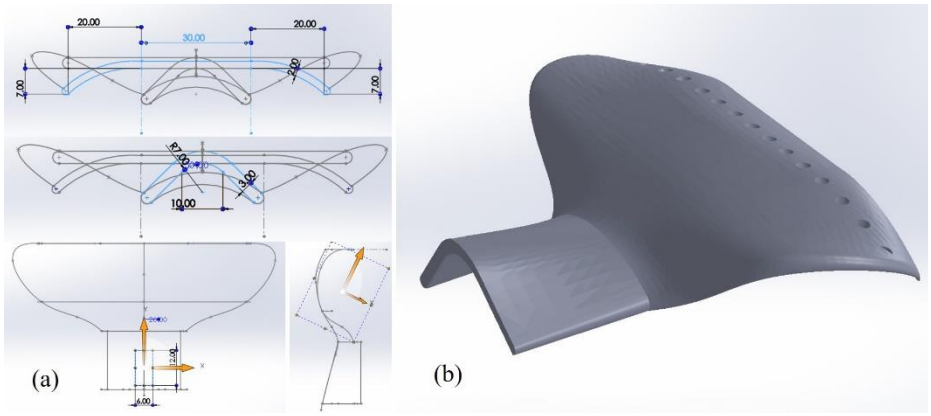

Figure 2. The design of the 3D-printed non-invasive reference marker based on anthropometry. T-shaped base contained a part of the eyebrow, glabella, and nasal bone (a). A patient-specific reference marker base was made to combine this T-shaped base with the CT image of the patient and created using the stereolithography 3D printer (b).

The separable frame was attached to the 3D-printed reference marker base, which was manufactured by 3D printing (Fabpro 1000, South Carolina, USA) (Fig. 3).[44] The frame consisted of two separable parts: one part (20 x 6 x 5 mm) fixed the frame itself to the reference marker base or the bone; the other part (12 x 6 x 6 mm) was used to insert or detach the EM tracking tool. Complementary shapes meant that the tracking tool could be combined in only one position and orientation.[44] As a result, the EM tracking tool and the reference marker base were always combined in the same geometrical relationship in attaching and repeatedly detaching during surgery.

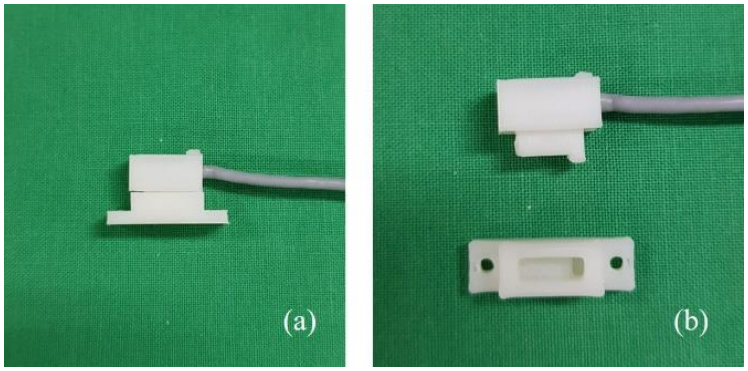

Figure 3. The separable frame for installing the EM tracking tool on the reference marker base (a) consists of two separable parts (b). Complementary shapes of parts mean that the tracking tool (EM sensor) could be combined in the same geometrical position.

3. Improved registrations using the registration body complex and 3D depth camera

The two registrations between the physical (EM tracking) and the CT image spaces and between the physical (EM tracking) and the AR camera spaces were performed preoperatively entirely using the registration body complex and 3D depth camera, which greatly simplified the workflow for the AR-assisted orthognathic surgery. The registration body complex consisted of the dental splint, the registration body, and the AR plane marker (Fig. 4, 5).

The dental splint was made from orthodontic self-curing acrylic resin.

The handle was made at the front of the dental splint, and the Lego blocks were placed on the top and the bottom of it. The dental splint would have three functions: connected the tracking EM sensor in the location, connected the registration body and the AR plane marker for registration, and was used to adjust the final occlusion as used in the conventional surgery.

The registration body is a symmetrical resin arch (Fig. 4) and embedded 22 ceramic spheres (1 mm in diameter) and six of these were selected to use as fiducial markers for registration. The registration body was made wide enough to include the upper and lower dentitions. At the bottom of the registration body, a Lego block (Lego Group, Billund, Denmark) was attached so that the registration body could be attached to the dental splint in the same positional relationship.[44]

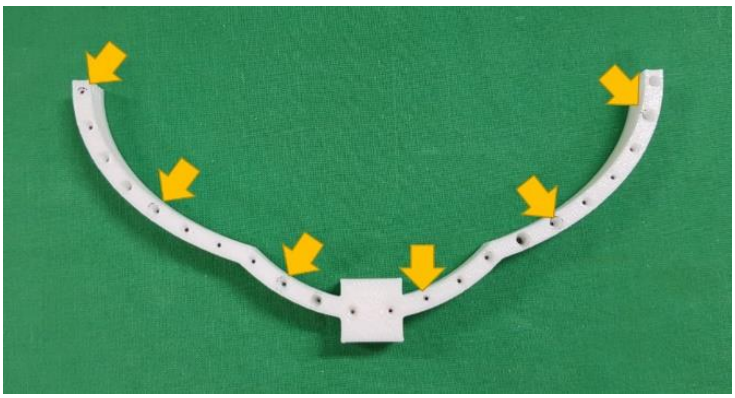

Figure 4. The registration body which is in the form of embedded 22 ceramic spheres and wide enough to include the dentitions. Six of these spheres (by arrows) were selected as fiducials for registration.

The AR plane marker with 55-mm edges is a plate form with a camera-recognizable marker tag and has four holes that can digitize the four vertex points of the marker tag accurately (Fig. 5).

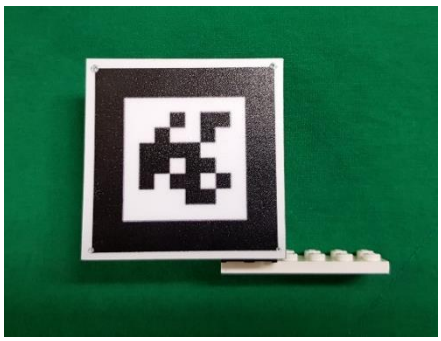

Figure 5. The AR plane marker is a plate form with a camera-recognizable marker tag. It has four holes on the vertex points of the marker tag that can be digitized. Point-to-point registration allowed it to connect the physical spaces of the actual patient and the AR camera spaces.

The AR registration and visualization were implemented using 2D and 3D information provided by the 3D depth camera. The intrinsic parameters of the camera were calibrated using a calibrator of MATLAB (MathWorks, Massachusetts, USA) and a checkerboard. The 3D virtual objects were superimposed on the real patient image by the camera using VTK (Visualization Toolkit, Kitware Inc., New York, USA) in real-time. The 3D coordinates of objects were reconstructed from the 2D pixel position of image coordinates by applying a pin-hole camera model using the camera SDK.

First, the registration between the physical and the CT image spaces was performed by point-to-point matching using the fiducial markers on the registration body (Fig. 6(a)). The physical positions of the fiducial markers on the registration body were measured with respect to the base EM tracking tool by applying an EM pointing tool. Aa a result, the affine transformation was determined by the registration between the patient's physical and the CT image spaces (M_{reg1} in Equation (2)).[8,34,44] These procedures could be performed before the surgery.

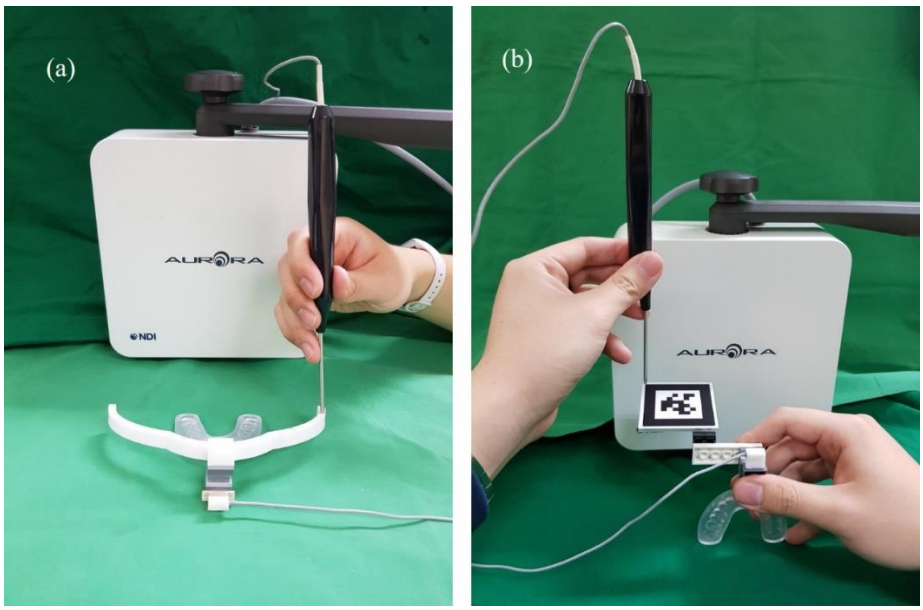

Figure 6. The preoperative registration was performed by measuring the position of the ceramic spheres on the registration body (a) and the four holes of the vertex points on the AR plane marker (b). The relative positions were recorded with respect to the base EM tracking tool by applying a pointing tool.

Second, the registration between the physical and the AR camera spaces was also performed by point-to-point matching using the four rectangular vertices on the AR plane marker. The physical positions of the four holes of vertex points on the AR plane marker were measured and recorded with respect to the base EM tracking tool by applying an EM pointing tool (Fig. 6(b)). The above procedure could be performed before surgery in a laboratory. In the operation room, the image of the marker tag was obtained by the depth camera and with this 2D coordinates and the *Z* coordinate value of the AR plane marker automatically recognized, the 3D coordinates of the AR plane marker in AR camera spaces are extracted using the following (Equation 1):

$$\gamma \begin{pmatrix} x \\ y \\ 1 \end{pmatrix} = \begin{pmatrix} f_x & 0 & c_x & 0 \\ 0 & f_y & c_y & 0 \\ 0 & 0 & 1 & 0 \end{pmatrix} \begin{pmatrix} X \\ Y \\ Z \\ 1 \end{pmatrix} \quad (1)$$

γ : scaling factor; *f*: focal length; *c*: principal point

x, *y*: 2D coordinates of the vertex point of marker tag from camera

Z: z coordinate of the vertex point of marker tag from the depth map

X, *Y*: 3D coordinates of the vertex point of marker tag by calculated

Moreover, point-to-point registration between the 3D coordinates extracted from the camera and EM tracking system was performed. (Fig. 7)

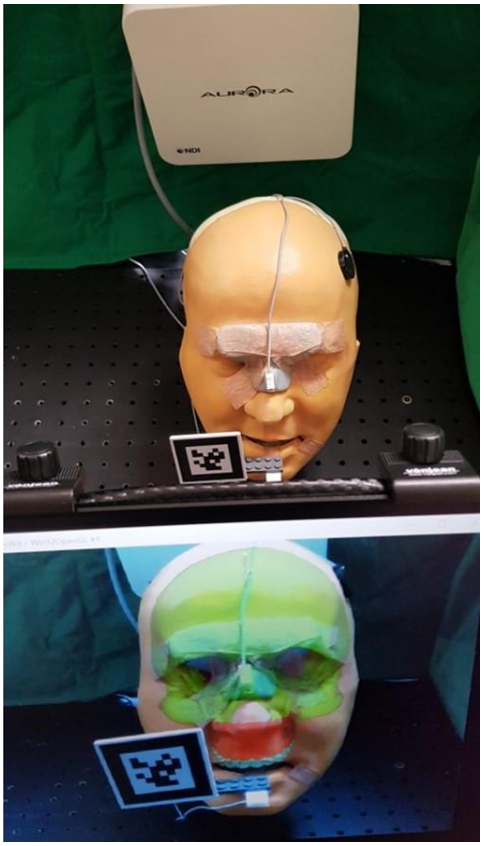

Figure 7. The immediate intraoperative registration in an operating room with the AR plane marker. The splint with the AR plane marker and the base EM tracking tool was attached to the patient. Only when the camera obtained the image of the AR plane marker, the registration was automatically completed.

The registration between the physical spaces using EM tracking and the AR camera spaces was determined immediately when the 3D coordinate of vertex points of the AR marker was determined automatically by the AR depth camera (M_{reg2} in Equation (2)).

4. Free hand AR surgical navigation system using quantitative visualization

When the AR plane marker was combined with the splint and the base EM tracking tool at the patient's dentition, the intraoperative registration between the physical and the AR camera spaces was also completed immediately by using the preoperative recording of the physical positions of the four marker vertices. Then, the AR plane marker was removed from the splint, and the bone segment could be tracked using only the EM tracking tool without the AR plane marker in the following AR visualization. The AR plane marker caused a line-of-sight obstruction intraoperatively in the same way as an optical tracking marker, which was solved by using only an EM tracking tool in this study.

Before starting the surgery, an EM reference marker was fixed to the patient's skull to exclude errors caused by the movements of the patient's head during surgery. When the splint with the base EM tracking tool was attached at the patient's dentition, the intraoperative registration between the physical and the CT image spaces was completed immediately by using the preoperative registration result.[8,44] Then, the relative position of the reference marker ($T_{ref\_0_{init}}$ in Equation (2)) at the patient's skull was recorded with respect to the base EM tracking tool ($T_{track_{init}}$ in Equation (2)) so that the reference marker could be used as a reference point in the following tracking (Equation 2).

$$T_{track\_camera} = M_{reg2} M_{reg1} \left({T_{ref\_0_{init}}}^{-1} T_{track_{init}} \right)^{-1} {T_{ref_{curr}}}^{-1} T_{track_{curr}} \quad (2)$$

T_{track_camera}: the current position of the maxilla segment in AR camera space

T_{ref_init}: the initial position of the reference marker in physical space

T_{track_init}: the initial position of the tracking marker in physical space

T_{ref_curr}: the current position of the reference marker in physical space

T_{track_curr}: the current position of the tracking marker in physical space

The overall procedure for AR surgical navigation for Le Fort I surgery was as followed (Fig. 8). (1) The intraoperative preparation was completed immediately using the registration body complex and software processing. (2) Le Fort I osteotomy was performed on the patient after removing the splint from the patient's dentition and the tracking tool of reference marker. (3) After osteotomy, the patient was recombined with the splint and the tracking tool of reference marker, and the corporate maxillary bone segment (MBS) and the reference marker were tracked by the EM tracking system (Equation (2)). The tracking tool could be separated from and recombined with the reference marker base repeatedly. (4) The movement of the intraoperative MBS was visualized on the AR display monitor by superimposition on the patient's image continuously in real-time while the MBS was handled freely by a surgeon for repositioning.

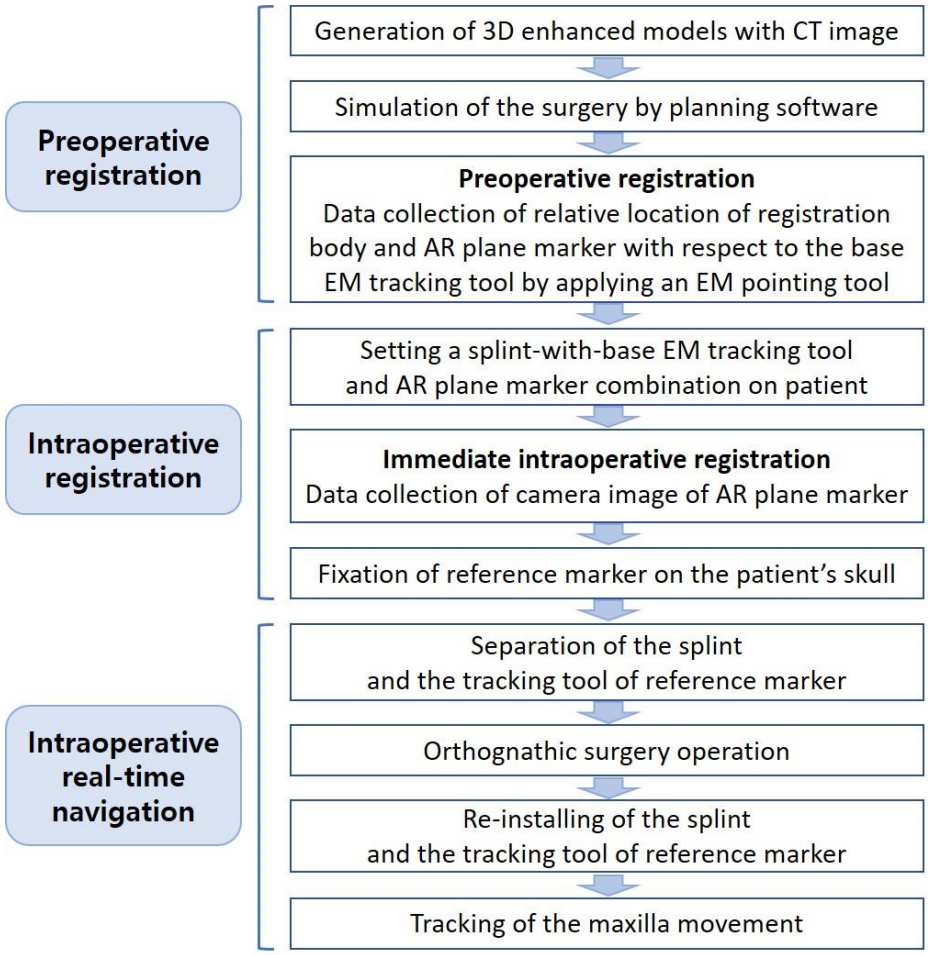

Figure 8. The whole procedure for the real-time AR surgical navigation system developed for Le Fort I surgery.

During repositioning, the intraoperative MBS model was visualized on the monitoring screen with respect to the goal MBS model simulated by the planning. The current model was expressed in a different color from the goal model. Also, the position of the selected surgical landmarks on the MBS model was calculated in the same way during repositioning because the models and the surgical landmarks comprised one rigid body. The current surgical landmark positions were also visualized on the MBS model during repositioning. That is, the positions of the multiple surgical landmarks of interest could be traced simultaneously during repositioning. Because the goal positions of the surgical landmarks had also been determined in advance, the deviation errors between the current and the planned positions of the landmarks could be calculated during repositioning. The 3D difference of the surgical landmarks was visualized numerically, which represented the quantified deviation error to the surgeon directly without applying a pointing tool to the patient during AR-assisted navigation surgery (Fig. 9). When a surgeon decided that the MBS had reached the final goal position and no more adjustment was required, the MBS was fixed to the skull and the deviation error between the present and the goal positions of the surgical landmarks was saved.

Figure 9. The tracking tool part of the reference marker base was reinstalled, and the splint-with-the EM tracking marker was attached to the patient to check the movement of maxillary bone segment. In this state, the location information for the maxillary bone segment was provided quantitatively and visually on AR flat-panel display. The coordinate deviations of the surgical landmarks between the planned and tracking positions were shown on the right side of the AR display.

5. Accuracy evaluation of AR surgical navigation system

5-1. Evaluation of registration accuracy of the AR surgical navigation system: target registration error (TRE)

To measure TRE, ten ceramic spheres were located on the phantom to use as anatomical target landmarks, which were at the pogonion, and the apical region of the bilateral upper canine, the bilateral lower canine, between the upper second premolar and the first molar, between the upper incisors, and between the lower second premolar and first molar (Fig. 10(a)). After registration using the registration body, an EM pointing tool was applied to the anatomical target landmarks directly (Fig. 10(b)), which were performed five times. The TRE was calculated by the root mean square (RMS) distance between actual and measured positions of the target landmarks.

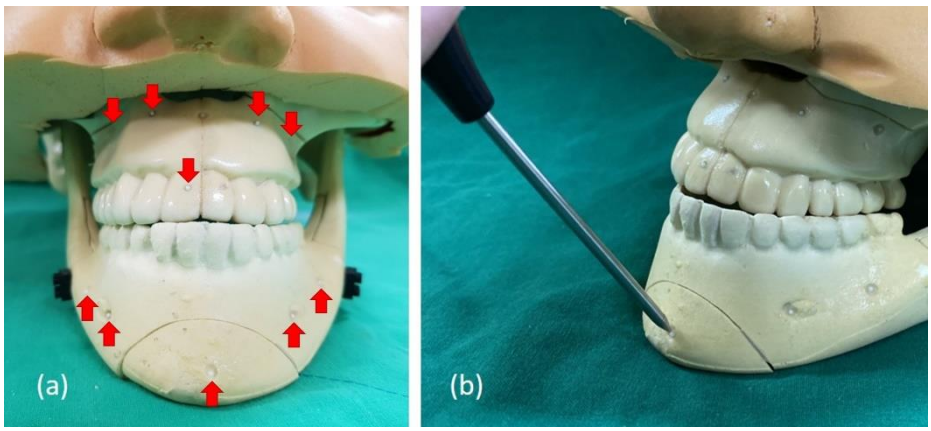

Figure 10. Ten ceramic spheres which are at the pogonion, and the apical region of the bilateral upper canine, the bilateral lower canine, between the upper second premolar and the first molar, between the upper incisors, and between the lower second premolar and first molar were used as anatomical target landmarks (a) to evaluate the target registration error values of the AR surgical navigation system. The coordinates of these target landmarks were obtained by applying an EM pointing tool (b).

Three reference markers were prepared to compare the accuracy of the 3D-printed non-invasive reference marker developed in this study and the other markers. The 3D-printed skin-attached non-invasive reference marker (NRM) that was manufactured (Fig. 11(a)), the reference marker that was fixed directly over the zygoma with bone screws (BRM_Z) (Fig. 11(b)), and the reference marker that was placed on the forehead with bone screws (BRM_F) (Fig. 11(c)) was placed on the phantom.

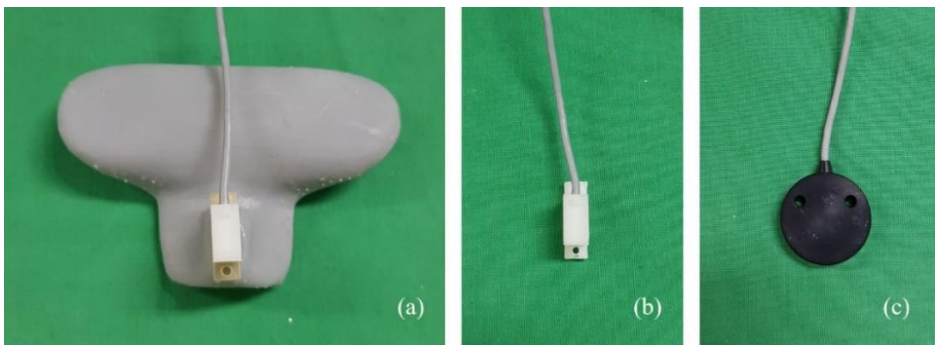

Figure 11. Three reference markers were used: (a) Developed 3D-printed patient-specific, non-invasive and skin-attached reference marker (NRM) for non-invasive approach, (b) invasive bone fixed reference marker in zygoma (BRM_Z) in a conventional method, (c) invasive bone fixed reference marker on forehead (BRM_F) in a conventional method.

5-2. Analysis of the accuracy of AR surgical navigation and the fixability of the 3D-printed non-invasive reference marker by performing Le Fort I surgery

Using a method developed previously, the planning simulation of the Le Fort I surgery was performed by applying the desired amount of displacement to the planning surgical landmarks which be selected directly on the teeth of the virtual maxillary model (Fig. 12).[8,44] The MBS model in planning software was set the coordinate system by contact point between the maxillary incisors, upper right first molar and canine, upper left canine and first molar, and PNS as the reference point. After finishing the surgical planning using the virtual maxillary model, the resulting displacements were applied to the virtual maxillary model to simulate the final postoperative position. To simulate the final postoperative positions of the landmarks, six surgical landmarks on the teeth (the right first molar, right canine, right incisor, left incisor, left canine, and left first molar) of the maxillary model was selected, and the same displacements resulting from the planning was also applied to those landmarks. During AR-assisted surgery, the deviation error between surgical landmark positions on the intraoperative was visualized, and the maxillary models were simulated quantitatively.

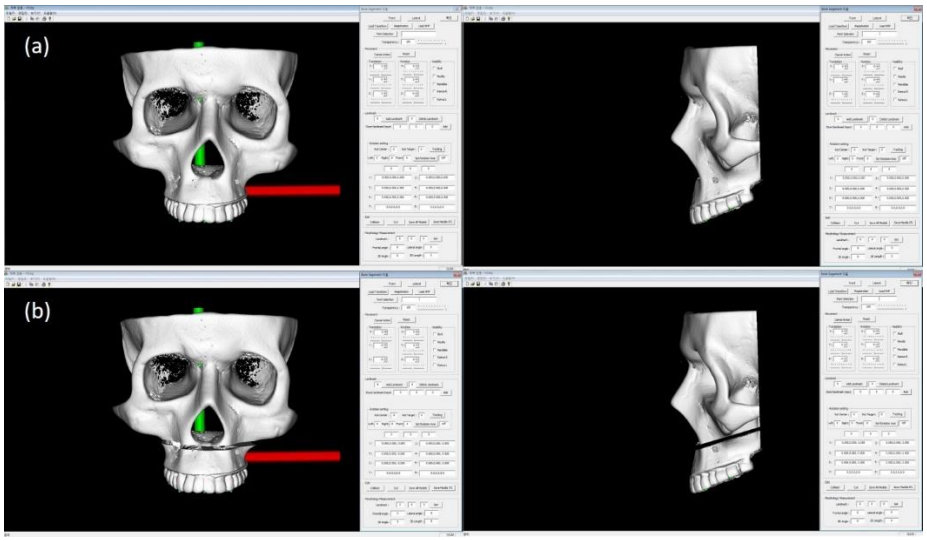

Figure 12. The surgical planning software using the 3D virtual skeletal enhanced model. (a) Pre-planned 3D enhanced model, (b) 3D enhanced model that moved the maxilla segment as planned (3 mm downward).

To evaluate the accuracy of the Le fort I surgery, a total of nine repositions of the maxillary bone segment were simulated by planning (Fig. 9). The bone segment was repositioned linearly by six translational movements of +3 mm and -3 mm in x-, y-, and z-axes directions respectively, which were in left lateral, right lateral, setback, advance, upward, and downward directions in the phantom's CT image space. The bone segment was also repositioned angularly by three rotational movements of 3 mm, which were roll (pivot the

right first molar 3-mm downward from left canine which is a central point), pitch (pivot the incisal contact point of central incisors 3-mm downward from PNS), yaw (pivot the incisal contact point of central incisors 3-mm right shift from PNS) orientations. BRM_Z and BRM_F were also set for comparison with the 3D-printed non-invasive reference marker (NRM). NRM was set as the gold standard that was used as the reference marker for the Le Fort I surgery of the phantom.

In order to simulate the condition of an actual surgery, the phantom skull was moved at various orientations by using the ball-socket joint after removing the splint with the EM tracking tool and the tracking tool of the reference marker during the Le fort I osteotomy. Then, the MBS was repositioned to the goal position after reattaching the splint and the tracking tool of the reference marker. The final postoperative positions of surgical landmarks were recorded automatically after fixing MBS. Each repositioning surgery was performed five times. The RMS and the absolute differences between the planned and postoperative positions at six landmarks on the maxillary teeth were calculated. The coordinates of surgical landmarks based on BRM_Z and BRM_F, which were not displayed on the screen during the operation, were also saved at the same time by tracking.

5-3. Statistical Analysis

For errors in the *x*, *y*, and *z* directions of the results, the RMS deviation was calculated to obtain the TRE value and between the planned position and the postoperative position. (Equation 3)

$$\sqrt{(x - x_0)^2 + \left(y - y_0\right)^2 + (z - z_0)^2} \qquad (3)$$

(x, y, z): final position of target landmark
(x_0, y_0, z_0): planned position of target landmark

Through the mean value of this deviation, the accuracy of the system was determined. The results between the three reference markers were tested for significance through ANOVA with the confidence of $p < 0.05$.

RESULTS

In this study, skull phantom was used to measure the TRE to evaluate the accuracy of the AR surgical navigation system with the 3D-printed non-invasive reference marker, and compared to the reference marker (be fixed in zygoma, and on forehead with bone screw) initially used. The TRE values showed that NRM was 0.88 ± 0.43, BRM_Z was 0.85 ± 0.39, and BRM_F was 0.94 ± 0.44 mm. Moreover, no significant difference was found between the three reference markers ($p > 0.05$).

Table 3. Comparison of TRE measurement between the three reference markers; 3D-printed non-invasive skin-attached, invasive bone-fixed reference marker in the zygoma, and invasive bone-fixed reference marker on the forehead.

	NRM (mm)	BRM_Z (mm)	BRM_F (mm)	*P*-value[†]
X	0.38 ± 0.34	0.39 ± 0.31	0.49 ± 0.39	
Y	0.31 ± 0.27	0.25 ± 0.23	0.30 ± 0.29	
Z	0.62 ± 0.41	0.60 ± 0.42	0.59 ± 0.44	
RMS	0.88 ± 0.43	0.85 ± 0.39	0.94 ± 0.44	0.449

NRM: skin-attached non-invasive reference marker
BRM_Z: invasive bone-fixed reference marker in the zygoma
BRM_F: invasive bone-fixed reference marker on the forehead
[†]*P*-value was calculated using One-way ANOVA.

The experiment of performing the Le Fort I surgery on the phantom using the developed AR surgical navigation system was conducted with a 3D-printed non-invasive reference marker as a gold standard. The virtual surgery planning was performed by the planning software (Fig. 12). When the AR surgical navigation system was performed in the operation stage, the 3D enhanced model-guided navigation monitor displayed quantified data and visualized form for the location information of segmentation (Fig. 13). Quantified data showed the difference between planned and current position of surgical landmark 1-6 (upper right first molar, upper right canine, upper right incisor, upper left incisor, upper left canine, upper left first molar) in the maxilla segment, and visualized form was developed so that three orthogonal planes (frontal, left horizontal, and transversal view) of real-time 3D enhanced model display could be printed on the monitor. The current position of the segment was indicated by grey color and the planned position by red color. When this position was matched, the two colors are merged and became a blur of pink color. In surgical landmark 1-6, the current position was displayed in sky blue dots and the planned position in red on display. When this position was matched, the color of the surgical landmark was shown as blue.

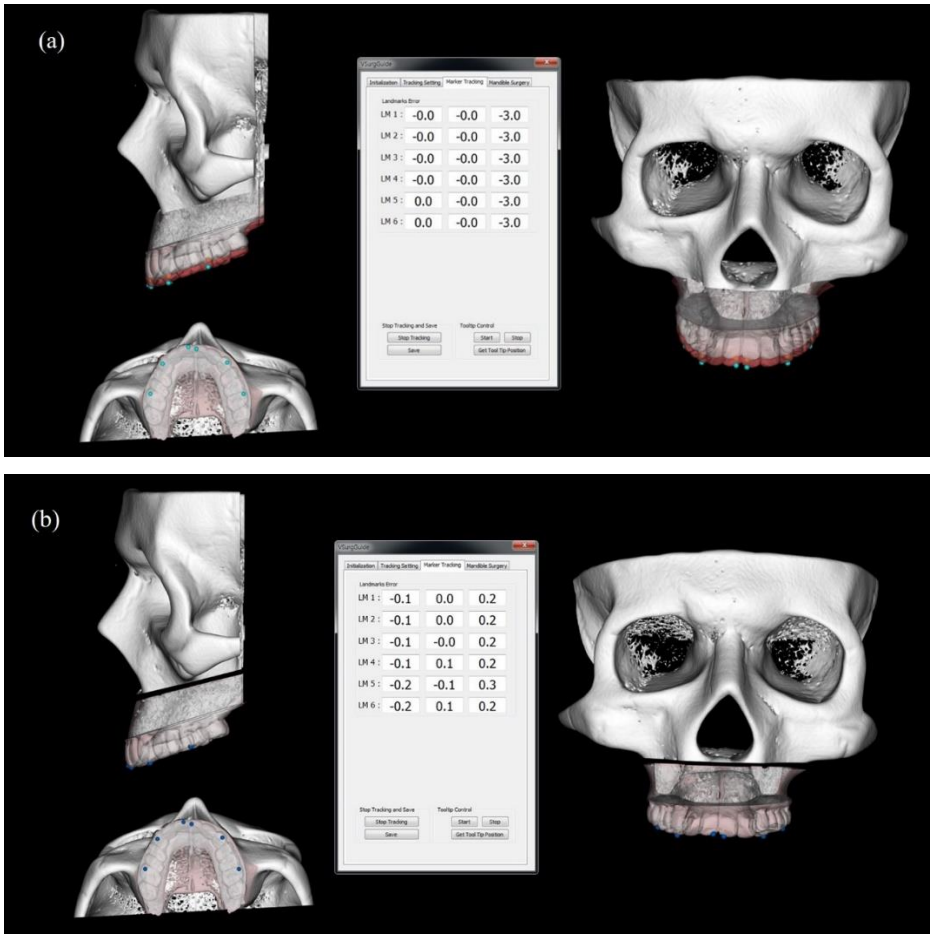

Figure 13. The monitor of the 3D enhanced model-guided navigation system displayed quantified data and visualized form. Quantified data showed the difference between the planned and current position of surgical landmarks 1-6. In visualized form, the current position of the maxilla segment was indicated by grey color, and the planned position was indicated by red color; displays before surgery (a), and after surgery (b).

The AR flat-panel display provided information by overlapping the virtual object above the real-time camera image (Fig. 14). By default, the maxilla model and the surgical landmarks of the 3D enhanced model visualized on the monitor. The model that was currently tracking was set to sky blue, and the model moved to a planned position was set to red. The occlusal plane was generated using the upper bilateral incisors, canines, and first molars to provide the information about canting correction to the surgeon. Moreover, the skull (green) and a vertical axis of the skull also visualized on the screen. All provided virtual objects were able to turn on or off according to the necessities of the surgeon, and the transparency was able to adjust. Also, for the surgery convenience, on the right side of the flat-panel display, the coordinate deviations of the surgical landmarks were provided quantitatively.

RMS results from each reference marker for surgery in nine directions were shown in Table 4. The total positional shift of the surgical results was 0.55 ± 0.14 mm, and no significant difference was found between the three reference markers; 3D-printed non-invasive reference marker, bone fixed reference marker in zygoma, bone-fixed reference marker in forehead ($p > 0.05$) (Table 5).

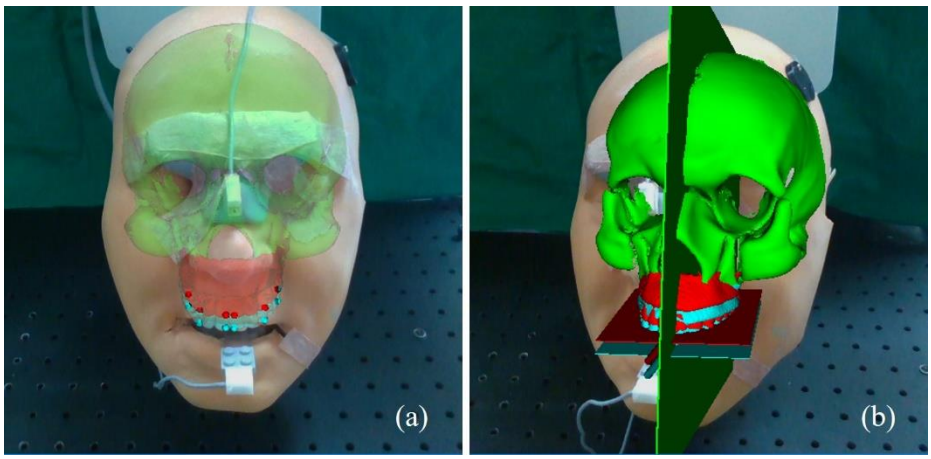

Figure 14. The flat-panel display provided the information by overlapping the virtual object the real-time AR camera image. All provided virtual objects were able to turn on or off according to the necessities of the surgeon, and the transparency was able to adjust. This image displayed the information of planned (red) and tracking position (sky-blue) of the maxillary bone segment, and the skull (green) with high transparency, and the six surgical landmarks of the 3D maxillary model (a). The occlusal plane and the vertical axis of the skull also visualized on the screen with low transparency (b).

Table 4. The difference in the x-, y-, and z-axes and RMS deviations between the planned and final postoperative position measured by the coordinate value of six surgical landmarks after nine orthognathic surgeries using AR surgical navigation system with 3D-printed non-invasive reference marker (unit: mm).

Types of surgeries	x	y	z	RMS
Left lateral (3mm)	0.22 ± 0.13	0.34 ± 0.11	0.26 ± 0.08	0.55 ± 0.23
Right lateral (3mm)	0.18 ± 0.08	0.45 ± 0.13	0.24 ± 0.16	0.62 ± 0.12
Setback (3mm)	0.22 ± 0.05	0.46 ± 0.11	0.28 ± 0.05	0.60 ± 0.10
Advance (3mm)	0.15 ± 0.07	0.25 ± 0.17	0.46 ± 0.17	0.60 ± 0.09
Upward (3mm)	0.13 ± 0.09	0.29 ± 0.10	0.38 ± 0.21	0.54 ± 0.12
Downward (3mm)	0.29 ± 0.14	0.27 ± 0.10	0.20 ± 0.07	0.50 ± 0.14
Roll (3mm)	0.20 ± 0.15	0.28 ± 0.17	0.18 ± 0.12	0.46 ± 0.08
Pitch (3mm)	0.18 ± 0.11	0.52 ± 0.16	0.16 ± 0.05	0.61 ± 0.16
Yaw (3mm)	0.26 ± 0.11	0.19 ± 0.13	0.35 ± 0.11	0.51 ± 0.19
	0.20 ± 0.10	0.34 ± 0.13	0.29 ± 0.11	0.55 ± 0.14

Table 5. Comparison of RMS deviation between each reference marker; 3D-printed non-invasive skin-attached, invasive bone-fixed reference marker in the zygoma, and invasive bone-fixed reference marker on the forehead.

	NRM	BRM_Z	BRM_F	*P*-value[†]
RMS (mm)	0.55 ± 0.14	0.54 ± 0.16	0.60 ± 0.16	0.08

NRM: skin-attached non-invasive reference marker
BRM_Z: invasive bone-fixed reference marker in the zygoma
BRM_F: invasive bone-fixed reference marker on the forehead
[†]*P*-value was calculated using One-way ANOVA.

DISCUSSION

The use of navigation technologies provided substantial improvement regarding the safety, aesthetic, and functional aspects in surgical procedures, such as dental implantology, arthroscopy of the temporomandibular joint, osteotomies, and distraction osteogenesis.[188] The image-guided systems for orthognathic surgery also facilitate increased reliability, flexibility, accuracy, and compatibility.[189,190] The imaging modalities and software have been improved so that the 3D virtual skeletal model-guided surgery system can be widely used to improve surgical outcomes. This model is manufactured by fusing the 3D representation of a CT dataset with an artifact-free high-resolution model of the dentitions,[180-182] using which the applied model is able to include accurate information of the dental surface.[180,191] The 3D model-guided orthognathic surgery system was effective in simulating the surgical treatment plan and reflecting it upon the actual surgery using navigation with high accuracy.[19,113]

When using the 3D virtual skeletal model in a navigation system for orthognathic surgery, the system works by visualizing the difference between the current position and the planned position of the bone segment and providing the relevant information accordingly. There are two methods for obtaining the quantified information in these surgeries. First, after the landmark on the region

of interest is digitized by applying a pointing tool, wherein the information of a single landmark can be obtained by one point.[16,17,33,113,192-194] Second, the system considers the skeletal segment to be a whole solid mass, where the quantified translational and rotational information of the segment is obtained numerically during free-hand surgery.[15,18,41,43,58] However, the system only shows the overall movement of the bone segment and it is difficult to quantify the error information of the specific anatomical region of interest.

Previously, an 3D enhanced model-guided orthognathic surgery system was developed to overcome these shortcomings in the 3D model-guided surgery system.[34,44] The intraoperative skeletal model with multiple surgical landmarks was visualized simultaneously on the monitor with respect to the simulated goal model, and the deviation errors between the intraoperative and the final goal positions of each landmark were also visualized quantitatively.[34,44] As a result, the surgeon could quickly determine the amount and direction of further bone movements needed to reach the goal position without applying a pointing tool, even when the operator is using a free hand.[34,44]

Due to the development of high-quality medical images, the navigation was applied in the medical field using AR, to facilitate the processing of the patient's virtual information on the image of the actual patient.[195] However, in the previous 3D enhanced model-guided surgery system,

the information was displayed on a monitor that was separate from the surgical sit , which caused difficulties in the surgeon's hand-eye coordination. To overcome this problem, the present AR surgical navigation system used a flat-panel display that enabled a surgeon to see this information at the right location. In the AR-assisted surgery, the surgeon was able to perform orthognathic surgery without losing attention from the surgical site, instruments, and procedures. This method showed the amount and direction of the bone movement needed to reach the goal position by superimposing an intraoperative skeletal model and landmarks with respect to the simulated goal model *in situ* on the surgical site of the patient. In addition to this, the rotation information, including canting of the bone segment, was provided intuitively to the surgeon by generating visuals of the current and planned positions of the occlusal plane and the mid-sagittal plane. As a result, the surgeon could perform Le Fort I surgery with precise hand-eye coordination and without losing any attention from the surgical site, instruments, and procedures.

As a substitute to conventional standing monitor of 3D model-guided surgery system,[81,84-86] numerous options have been used for visualization device of the AR-assisted system such as head-mounted device (HMD), half-silvered mirror, flat-panel monitor. Although the HMD based system is the most classical use of AR, this system has many drawbacks: inattentional blindness by using the small size of the screen,[81] focus problem caused by operative field

and the display are not projected on the same plane when using the see-through projection, and the heavy and bulky devices to wear. Due to these reasons, flat-panel monitor based systems were considered in this study. However, it could also arise an asthenopia (eye strain) associated with concentrating on a screen for a long time,[97] and the virtual object reduces the visibility of the surgical site and important structures.[48] The virtual information of the developed AR-assisted surgery system was overlaid only when the surgeon required and not throughout the procedure to reduce shortcomings.

An AR surgical method consisting of a portable display and an optical tracking system showed superimposed virtual models of the patient's face on the image for computer-assisted Le Fort I surgery.[33,92] The potential of this technique was shown from the perspective of a surgical assistant by reproducing the Le Fort I orthognathic procedure in a phantom skull.[68] However, no quantitative information was provided during surgery in these AR-assisted methods. Therefore, the developed method in the present study enabled surgeons to perform the free-hand orthognathic surgery intuitively and comfortably with precise hand-eye coordination, based on the quantitative and qualitative visualization of AR in real-time.

In this study, to simplify the workflow of the AR surgical navigation system, the registration body complex and a 3D depth camera were used. The registration process consists of complete preoperative registration and

immediate intraoperative registration. Most of the registration procedures were performed before surgery in a laboratory. The registration method has better accuracy when the distance between the position of the tracking target and the location of the registration fiducials is kept shorter,[46] since the distance between the registration fiducial (ceramic sphere) and the maxilla segment is very small and the accuracy in this case is good. The advantage of preoperative registration is that the surgeon can perform it almost completely before the surgery, without needing to observe the patients simultaneously. This reduces the surgeon's effort in performing the entire registration process in the operating room. Intraoperative registration was performed automatically and immediately by obtaining depth information from the 3D depth camera. The improved registration allowed the physical (using the EM tracking system), 3D model, and AR camera spaces to be matched. The developed method is unlike the conventional registration method because it minimized the cross-infection as it did not directly adhere to the patient's skin. Moreover, the developed method helped us to obtain accurate registration because it was not affected by the technical proficiency of the surgeon. Further, the process was minimally invasive and easy to use because it was applied by a splint method and followed a simplified workflow. It also reduced the overall surgery time and improved the accuracy of the surgical procedure.

Generally, the AR visualization was implemented by using an optical

tracking marker, which caused a line-of-sight obstruction intraoperatively. In this study, only an EM tracking tool was used, not using any optical tracking marker during the AR navigation orthognathic surgery. The optical tracking–based navigation system suffered from line-of-sight obstruction between the tracking tool and camera and the requirement for bulky tracking tools in local or minimally invasive surgeries.[43] The landmarks of optical reference profoundly influence the interest in the maxillofacial surgery area, which was pointed out as a limitation of AR, but this was overcome by the use of the EM tracking system. A navigation surgery system based on EM tracking has no line-of-sight problem and uses relatively small tracking tools, so it has been used in minimally invasive surgeries and to track internal organs.[30,36,41-43] In a previous study using the EM surgical navigation for MPS repositioning, the EM tracking tool was fixed securely and inseparably to the bone segment.[41] The EM tracking tool itself was connected by a cable with the tracking system. This feature could show many disadvantages, such as interference with the view of the surgeon, restriction of access, damage to the cable, increase in the surgical time and effort, and, in severe cases, breakdown due to iatrogenic accidents.[44] Although wireless sensors have been developed to address the disadvantages of the existence of cables, they are still not used in routine practice in EM navigation (especially in craniomaxillofacial surgery).[196,197] In this study, a separable frame was used, allowing to attach and separate the EM tracking tool

from the bone segment repeatedly. The AR-assisted surgery using separable frame could allow the surgeon to perform the orthognathic surgery with no line-of-sight obstruction and minimal interference by the connecting with a cable.

The development of a non-invasive surgical method is the aim of computer-aided surgery.[46] To non-invasively apply the image-guided navigation system, several fixed methods of the reference marker have been developed, including skin-adhesive markers, anatomic landmarks, oral splints, and laser scans,[39] however, the use of these methods were found to negatively affect the TRE.[137-141] Therefore, the registration method that employs the bone-fixed screw is still used as the gold standard.[143-146]

A 3D-printed non-invasive reference marker was developed for a novel, non-invasive AR surgical navigation system for orthognathic surgery. This marker was attached to the patient's skin during surgery. In the existing papers, many manipulation errors have been overlaid with low accuracy because skin-adhesive markers were used in the CT scanning and the registration method. Thus, in this study, the base EM tracking tool attached to the splint was used as a reference point during the registration process. Therefore, the reference marker was used as reference point by recording the relative position of the reference marker with respect to the base EM tracking tool just before the surgery, and after this process, the base EM tracking tool was used as a tracking marker. Owing to this process, the developed reference

marker did not undergo any manipulation errors till it was attached to the patient and the operation was completed. This indicates that the accuracy of the system was maintained throughout the procedure.

This 3D-printed non-invasive reference marker uses a separable frame to take the EM tracking tool off and attach it in an accurate position.[44] This reduces complications, such as infection or scarring, saves time, and is convenient to use. Further, there is no interference in the EM tracking system because it does not use metallic screws. However, a limitation of this non-invasive reference marker production process is that since 3D printing is used, each patient-specific marker needs to be manufactured individually and the accuracy can be reduced in the fabrication process using CT scanning and 3D printers. In addition, the developed reference marker is designed to be placed in a thin area so it can be firmly fixed with medical tape and is not significantly affected by the swelling that may occur during surgery. Also, this is possible because the sensor of the EM tracking system is very small and lightweight. However, further studies are needed to explore whether the reference marker will show a similar accuracy when applied to actual patients.

During the accuracy evaluation of the developed AR surgical navigation system, the results of the TRE showed an average value of 0.89 ± 0.42 mm (Table 3). The accuracy of the developed EM tracking system was deemed to be sufficient, since an accuracy of less than 1.5 mm is generally

recommended for typical computer-assisted surgery applications[28,198,199] and 1-2 mm accuracy is recommended for optical tracking systems.[10,200,201] Therefore, the findings indicate that the system developed by us could be a useful tool in clinical practice. The accuracy evaluation of the 3D-printed non-invasive reference marker was conducted by comparing it with the bone-fixed reference marker (zygoma & forehead). The TRE results of the 3D-printed non-invasive marker were almost similar to those of the bone-fixed reference marker (Table 3). It was found that, regardless of the fixed-ness of the reference marker, the TRE increased slightly as the distance of the registration fiducial marker from the zygoma, glabella, and forehead increased.

In a previous study, the RMS deviation of the translational displacements around the incisor point for the patients, as shown by the application of 16 actual clinical plans of orthognathic surgery, was obtained on an average measurement of 3 mm.[202] Based on this, for analyzing the accuracy and fixability of the 3D-printed non-invasive reference marker, it was decided that, in this study, the plan for the Le Fort I surgery was to move the relevant bone +3 mm and -3 mm, respectively, in the x, y, and z directions, and move it 3 mm each in the roll, pitch, and yaw directions. The Le Fort I surgery result showed that RMS (the mean value of deviation between the planned and final postoperative position) of the 3D-printed non-invasive reference marker was 0.55 ± 0.14 mm (Table 4). The success criterion has been mentioned by several

authors and refers to a maximum difference of 2 mm between the virtually planned surgical procedure and the actual outcome.[203-205] Other studies of 3D model-guided surgery systems conducted on Le Fort I surgery using a bone-fixed reference marker and based on an EM tracking system showed RMS deviations (total positional shift) of 1.1 mm[43] and 0.62 mm.[136] Moreover, earlier studies of AR-assisted surgery systems conducted on maxillofacial surgery using AR-assisted surgery system reports postoperative overall errors: the implant surgery performed on 3D printed mandibular models showed less than 1.5 mm as linear deviation,[61] the orbital reconstruction performed on 3D printed hard tissue model showed 1.12 – 1.15 mm as translation error,[59] and the maxillofacial surgery performed on plastic model showed 0.77 mm positional error.[59]

Moreover, the RMS deviation of the bone-fixed reference marker (zygoma and forehead) is simultaneously obtained after each operation to demonstrate the fixation of the 3D-printed non-invasive reference marker. The ANOVA tests showed no significant difference between the three reference markers (Table 5). In other words, the 3D-printed non-invasive reference markers developed in this study were found to be sufficiently fixed, enough to be able to replace the bone-fixed reference markers from an accuracy perspective.

Through the convergence of AR and VR, development of an integrated user interface system would be needed, that can provide a variety of information while ensuring reliability and accuracy while increasing intuition. In future studies, the developed AR navigation system will be applied to the actual orthognathic surgery in operating rooms and be analyzed for its surgical usability and accuracy.

CONCLUSION

An AR navigation system for orthognathic surgery using a flat-panel display, an EM tracking system, and a 3D-printed non-invasive reference marker was developed. The workflow of the AR navigation system was improved by using the simplified registration method and a 3D-printed non-invasive reference marker intraoperatively. And the evaluation of the developed system displayed acceptable accuracy. In future studies, this system needs to be applied to clinical experiment.

REFERENCES

1. Franz AM, Haidegger T, Birkfellner W, Cleary K, Peters TM, Maier Hein L. Electromagnetic tracking in medicine—a review of technology, validation, and applications. *IEEE Trans Med Imaging.* 2014;33(8):1702-1725.

2. Vávra P, Roman J, Zonča P, Ihnát P, Němec M, Kumar J, Habib N, El Gendi A. Recent development of augmented reality in surgery: a review. *J Healthc Eng.* 2017;2017:4574172.

3. Chen X, Xu L, Sun Y, Politis C. A review of computer-aided oral and maxillofacial surgery: planning, simulation and navigation. *Expert Rev Med Devices.* 2016;13(11):1043-1051.

4. Kersten Oertel M, Gerard I, Drouin S, Mok K, Sirhan D, Sinclair DS, Collins DL. Augmented reality in neurovascular surgery: feasibility and first uses in the operating room. *Int J Comput assist Radiol Surg.* 2015;10(11):1823-1836.

5. Rassweiler J, Rassweiler MC, Müller M, Kenngott H, Meinzer HP, Teber D. Surgical navigation in urology: European perspective. *Curr Opin Urol.* 2014;24(1):81-97.

6. Ward TJ, Goldman RE, Weintraub JL. Electromagnetic Navigation With Multimodality Image Fusion for Image-guided Percutaneous Interventions. *Tech Vasc Interv Radiol.* 2013;16(3):177-181.

7. Shim KB, Shin SH, Nam MS, Kim BY. Real-Time Navigation-Assisted Orthognathic Surgery. *J Craniofac Surg.* 2013;24(1):221-225.

8. Kim DS, Woo SY, Yang HJ, Huh KH, Lee SS, Heo MS, Choi SC, Hwang SJ, Yi WJ. An integrated orthognathic surgery system for virtual planning and image-guided transfer without intermediate splint. *J Craniomaxillofac Surg.* 2014;42(8):2010-2017.

9. Schramm A, Gellrich NC, Gutwald R, Schipper J, Bloss H, Hustedt H,

Schmelzeisen R, Otten JE. Indications for computer-assisted treatment of cranio-maxillofacial tumors. *Comput Aided Surg* 2000;5(5):343-352.

10. Hassfeld S, Mühling J. Computer assisted oral and maxillofacial surgery – a review and an assessment of technology. *Int J Oral Maxillofac Surg.* 2001;30(1):2-13.

11. Gellrich NC, Schramm A, Hammer B, Rojas S, Cufi D, Lagrèze W, Schmelzeisen R. Computer-assisted secondary reconstruction of unilateral posttraumatic orbital deformity. *Plast Reconstr Surg.* 2002;110(6):1417-1429.

12. Caversaccio M, Bächler R, Lädrach K, Schroth G, Nolte LP, Häusler R. The “Bernese” frameless optical computer aided surgery system. *Comput Aided Surg.* 1999;4(6):328-334.

13. O'Grady KF, Antonyshyn OM. Facial asymmetry: three-dimensional analysis using laser surface scanning. *Plast Reconstr Surg.* 1999;104(4):928-937.

14. De Momi E, Chapuis J, Pappas I, Ferrigno G, Hallermann W, Schramm A, Caversaccio M. Automatic extraction of the mid-facial plane for cranio-maxillofacial surgery planning. *Int J Oral Maxillofac Surg.* 2006;35(7):636-642.

15. Chapuis J, Schramm A, Pappas I, Hallermann W, Schwenzer-Zimmerer K, Langlotz F, Caversaccio M. A New System for Computer-Aided Preoperative Planning and Intraoperative Navigation During Corrective Jaw Surgery. *IEEE Trans Inf Technol Biomed.* 2007;11(3):274-287.

16. Bell RB. Computer planning and intraoperative navigation in cranio-maxillofacial surgery. *Oral Maxillofac Surg Clin North Am.* 2010;22(1):135-156.

17. Mazzoni S, Badiali G, Lancellotti L, Babbi L, Bianchi A, Marchetti C. Simulation-guided navigation: a new approach to improve intraoperative three-dimensional reproducibility during orthognathic surgery. *J Craniofac Surg.* 2010;21(6):1698-1705.

18. Li GFB, Zhang GFL, Sun GFH, Shen GFS, Wang GFX. A New Method of Surgical Navigation for Orthognathic Surgery: Optical Tracking Guided Free-Hand Repositioning of the Maxillomandibular Complex. *J Craniofac Surg.* 2014;25(2):406-411.

19. Chang HW, Lin HH, Chortrakarnkij P, Kim SG, Lo LJ. Intraoperative navigation for single-splint two-jaw orthognathic surgery: From model to actual surgery. *J Cranio Maxillofac Surg.* 2015;43(7):1119-1126.

20. Wang X, Truijens M, Hou L, Wang Y, Zhou Y. Integrating Augmented Reality with Building Information Modeling: Onsite construction process controlling for liquefied natural gas industry. *Automation Constr.* 2014;40:96-105.

21. Ricciardi F, Copelli C, De Paolis LT. An augmented reality system for maxillo-facial surgery. In. *Int Conf Augmented Reality Virtual Reality Comput Graph*: Springer; 2017:53-62.

22. Teber D, Guven EO, Baumhauer M, Simpfendörfer T, Rassweiler J. Augmented reality: a new tool to improve surgical accuracy during laparoscopic partial nephrectomy? Preliminary in vitro and in vivo results. *Eur Urol.* 2009;56(2):332-338.

23. Farronato M, Maspero C, Lanteri V, Fama A, Ferrati F, Pettenuzzo A, Farronato D. Current state of the art in the use of augmented reality in dentistry: a systematic review of the literature. *BMC Oral Health.* 2019;19(1):135.

24. Cutolo F, Siesto M, Mascioli S, Freschi C, Ferrari M, Ferrari V. Configurable software framework for 2D/3D video see-through displays in medical applications. *Int Conf Augmented Reality Virtual Reality Comput Graph.* 2016;9769:30-42.

25. Katić D, Spengler P, Bodenstedt S, Castrillon Oberndorfer G, Seeberger R, Hoffmann J, Dillmann R, Speidel S. A system for context-aware intraoperative augmented reality in dental implant surgery. *Int J Comput Assist Radiol Surg.* 2015;10(1):101-108.

26. Bettega G, Dessenne V, Raphael B, Cinquin P. Computer-assisted mandibular condyle positioning in orthognathic surgery. *J Oral Maxillofac Surg.* 1996;54(5):553-558.

27. Marmulla R, Mühling J, Lüth T, Hassfeld S. Physiological shift of facial skin and its influence on the change in precision of computer-assisted surgery. *Br J Oral Maxillofac Surg.* 2006;44(4):273-278.

28. Eggers G, Mühling J, Hofele C. Clinical use of navigation based on cone-beam computer tomography in maxillofacial surgery. *Br J Oral Maxillofac Surg.* 2009;47(6):450-454.

29. Zhang W, Wang C, Yu H, Liu Y, Shen G. Effect of fiducial configuration on target registration error in image-guided cranio-maxillofacial surgery. *J Cranio Maxillofac Surg.* 2011;39(6):407-411.

30. Seeberger R, Kane G, Hoffmann J, Eggers G. Accuracy assessment for navigated maxillo-facial surgery using an electromagnetic tracking device. *J Cranio Maxillofac Surg.* 2012;40(2):156-161.

31. Zhang W, Wang C, Shen G, Wang X, Cai M, Gui H, Liu Y, Yang D. A novel device for preoperative registration and automatic tracking in cranio-maxillofacial image guided surgery. *Comput Aid Surg.* 2012;17(5):259-267.

32. Kim SH, Kim DS, Huh KH, Lee SS, Heo MS, Choi SC, Hwang SJ, Yi WJ. Direct and continuous localization of anatomical landmarks for image-guided orthognathic surgery. *Oral Surg Oral Med Oral Pathol Oral Radiol.* 2013;116(4):402-410.

33. Zinser MJ, Mischkowski RA, Dreiseidler T, Thamm OC, Rothamel D, Zöller JE. Computer-assisted orthognathic surgery: waferless maxillary positioning, versatility, and accuracy of an image-guided visualisation display. *Br J Oral Maxillofac Surg.* 2013;51(8):827-833.

34. Lee SJ, Woo SY, Huh KH, Lee SS, Heo MS, Choi SC, Han JJ, Yang HJ, Hwang SJ, Yi WJ. Virtual skeletal complex model-and landmark-guided orthognathic surgery system. *J Cranio Maxillofac Surg.* 2016;44(5):557-568.

35. Savoldelli C, Chamorey E, Bettega G. Computer-assisted teaching of bilateral sagittal split osteotomy: Learning curve for condylar positioning. *PloS one.* 2018;13(4):e0196136.

36. Berger M, Kallus S, Nova I, Ristow O, Eisenmann U, Dickhaus H, Kuhle R, Hoffmann J, Seeberger R. Approach to intraoperative electromagnetic navigation in orthognathic surgery: a phantom skull based trial. *J CranioMaxillofac Surg.* 2015;43(9):1731-1736.

37. Muench RK, Blattmann H, Kaser Hotz B, Bley CR, Seiler PG, Sumova A, Verwey J. Combining magnetic and optical tracking for computer aided therapy. *Z Med Phys.* 2004;14(3):189-194.

38. Hummel J, Figl M, Birkfellner W, Bax MR, Shahidi R, Maurer Jr C, Bergmann H. Evaluation of a new electromagnetic tracking system using a standardized assessment protocol. *Phys Med Biol.* 2006;51(10):N205-210.

39. Grauvogel TD, Grauvogel J, Arndt S, Berlis A, Maier W. Is there an equivalence of non-invasive to invasive referenciation in computer-aided surgery? *Eur Arch Otorhinolaryngol.* 2012;269(10):2285-2290.

40. Schicho K, Figl M, Donat M, Birkfellner W, Seemann R, Wagner A, Bergmann H, Ewers R. Stability of miniature electromagnetic tracking systems. *Phys Med Biol.* 2005;50(9):2089-2098.

41. Berger M, Nova I, Kallus S, Ristow O, Eisenmann U, Dickhaus H, Engel M, Freudlsperger C, Hoffmann J, Seeberger R. Electromagnetic navigated condylar positioning after high oblique sagittal split osteotomy of the mandible: a guided method to attain pristine temporomandibular joint conditions. *Oral Surg Oral Med Oral Pathol Oral Radiol.* 2018;125(5):407-414.

42. Nova I, Kallus S, Berger M, Ristow O, Eisenmann U, Freudlsperger C, Hoffmann J, Dickhaus H. Computer assisted positioning of the proximal segment after sagittal split osteotomy of the mandible: Preclinical investigation of a novel electromagnetic navigation system. *J Cranio Maxillofac Surg.* 2017;45(5):748-754.

43. Lutz JC, Nicolau S, Agnus V, Bodin F, Wilk A, Bruant Rodier C, Rémond Y, Soler L. A novel navigation system for maxillary positioning in orthognathic surgery: preclinical evaluation. *J Cranio Maxillofac Surg.* 2015;43(9):1723-1730.

44. Lee SJ, Yang HJ, Choi MH, Woo SY, Huh KH, Lee SS, Heo MS, Choi SC, Hwang SJ, Yi WJ. Real-time augmented model guidance for mandibular proximal segment repositioning in orthognathic surgery, using electromagnetic tracking. *J Cranio Maxillofac Surg.* 2019;47(1):127-137.

45. Shamir RR, Joskowicz L, Shoshan Y. Fiducial optimization for minimal target registration error in image-guided neurosurgery. *IEEE Trans Med Imaging.* 2011;31(3):725-737.

46. Soteriou E, Grauvogel J, Laszig R, Grauvogel T. Prospects and limitations of different registration modalities in electromagnetic ENT navigation. *Eur Arch Otorhinolaryngol.* 2016;273(11):3979-3986.

47. Dey A, Billinghurst M, Lindeman RW, Swan J. A Systematic Review of 10 Years of Augmented Reality Usability Studies: 2005 to 2014. *Front Robot AI.* 2018;5:37.

48. Hussain R, Lalande A, Guigou C, Bozorg Grayeli A. Contribution of Augmented Reality to Minimally Invasive Computer-Assisted Cranial Base Surgery. *IEEE J Biomed Health Inform.* 2019;18.

49. Blackwell M, Morgan F, Digioia A. Augmented reality and its future in orthopaedics. *Clin Orthop Rel Res.* 1998(354):111-122.

50. Meola A, Cutolo F, Carbone M, Cagnazzo F, Ferrari M, Ferrari V. Augmented reality in neurosurgery: a systematic review. *Neurosurg Rev.* 2017;40(4):537-548.

51. Bastien S, Peuchot B, Tanguy A. Augmented reality in spine surgery. Critical appraisal and status of development. *Stud Health Technol Inform.* 2002;88:153-156.

52. De Paolis LT, Pulimeno M, Aloisio G. An augmented reality application for minimally invasive surgery. *Biomed Eng Med Phys.* 2008;20:489-492.

53. Marescaux J, Diana M, Soler L. Augmented reality and minimally invasive surgery. *J Gastroenterol Hepatol Res.* 2013;2(5):555-560.

54. De Paolis LT, Ricciardi F, Dragoni AF, Aloisio G. An augmented reality application for the radio frequency ablation of the liver tumors. *Int Conf Comput Sci App.* 2011;6785:572-581.

55. Murugesan YP, Alsadoon A, Manoranjan P, Prasad PWC. A novel rotational matrix and translation vector algorithm: geometric accuracy for augmented reality in oral and maxillofacial surgeries. *Int J Med Robot Comput Assist Surg.* 2018;14(3):e1889.

56. Qu M, Hou Y, Xu Y, Shen C, Zhu M, Xie L, Wang H, Zhang Y, Chai G. Precise positioning of an intraoral distractor using augmented reality in patients with hemifacial microsomia. *J Cranio Maxillofac Surg.* 2015;43(1):106-112.

57. Wang J, Suenaga H, Yang L, Kobayashi E, Sakuma I. Video see-through augmented reality for oral and maxillofacial surgery. *Int J Med Robot Comput Assist Surg.* 2017;13(2).

58. Mischkowski RA, Zinser MJ, Ritter L, Neugebauer J, Keeve E, Zöller JE. Intraoperative navigation in the maxillofacial area based on 3D imaging obtained by a cone-beam device. *Int J Oral Maxillofac Surg.* 2007;36(8):687-694.

59. Suenaga H, Hoang Tran H, Liao H, Masamune K, Dohi T, Hoshi K, Mori Y, Takato T. Real-time in situ three-dimensional integral videography and surgical navigation using augmented reality: a pilot study. *Int J Oral Sci.* 2013;5(2):98-102.

60. Zhu M, Chai G, Zhang Y, Ma X, Gan J. Registration Strategy Using Occlusal Splint Based on Augmented Reality for Mandibular Angle Oblique Split Osteotomy. *J Craniofac Surg.* 2011;22(5):1806-1809.

61. Jiang W, Ma L, Zhang B, Fan Y, Qu X, Zhang X, Liao H. Evaluation of the 3D Augmented Reality-Guided Intraoperative Positioning of Dental Implants in Edentulous Mandibular Models. *Int J Oral Maxillofac implants.* 2018;33(6):1219-1228.

62. Schreurs R, Dubois L, Becking AG, Maal TJJ. Implant-oriented navigation in orbital reconstruction. Part 1: technique and accuracy study. *Int J Oral Maxillofac Surg.* 2018;47(3):395-402.

63. Lin YK, Yau HT, Wang IC, Zheng C, Chung KH. A Novel Dental Implant Guided Surgery Based on Integration of Surgical Template and Augmented Reality. *Clin Implant Dent Relat Res.* 2015;17(3):543-553.

64. Bruellmann D, Tjaden H, Schwanecke U, Barth P. An optimized video system for augmented reality in endodontics: a feasibility study. *Clin Oral Investig.* 2013;17(2):441-448.

65. Wierinck ER, Puttemans V, Swinnen SP, van Steenberghe D. Expert performance on a virtual reality simulation system. *J Dent Edu.* 2007;71(6):759-766.

66. Aichert A, Wein W, Ladikos A, Reichl T, Navab N. Image-based tracking of the teeth for orthodontic augmented reality. *Med Image Comput Comput Assist Interv.* 2012;15:601-608.

67. Azuma RT. A Survey of Augmented Reality. *Presence: Teleoperators & Virtual Environments.* 1997;6(4):355-385.

68. Badiali G, Ferrari V, Cutolo F, Freschi C, Caramella D, Bianchi A, Marchetti C. Augmented reality as an aid in maxillofacial surgery: Validation of a wearable system allowing maxillary repositioning. *J Craniomaxillofac Surg.* 2014;42(8):1970-1976.

69. Freysinger W, Gunkel A, Thumfart W. Image-guided endoscopic ENT surgery. *Eur Arch Otorhinolaryngol.* 1997;254(7):343-346.

70. Wagner A, Millesi W, Watzinger F, Truppe M, Rasse M, Enislidis G, Kermer C, Ewers R. Clinical experience with interactive teleconsultation and teleassistance in craniomaxillofacial surgical

procedures. *J Oral Maxillofac Surg.* 1999;57(12):1413-1418.

71. Citardi MJ, Agbetoba A, Bigcas JL, Luong A. Augmented reality for endoscopic sinus surgery with surgical navigation: a cadaver study. *Int Forum Allergy Rhinol.* 2016;6(5):523-528.

72. Wagner A, Ploder O, Enislidis G, Truppe M, Ewers R. Virtual image guided navigation in tumor surgery — technical innovation. *J Cranio Maxillofac Surg.* 1995;23(5):271-273.

73. Wagner A, Rasse M, Millesi W, Ewers R. Virtual reality for orthognathic surgery: The augmented reality environment concept. *J Oral Maxillofac Surg.* 1997;55(5):456-462.

74. Bong JH, Song HJ, Oh Y, Park N, Kim H, Park S. Endoscopic navigation system with extended field of view using augmented reality technology. *Int J Med Robot.* 2018;14(2).

75. Inoue D, Cho B, Mori M, Kikkawa Y, Amano T, Nakamizo A, Yoshimoto K, Mizoguchi M, Tomikawa M, Hong J, Hashizume M, Sasaki T. Preliminary study on the clinical application of augmented reality neuronavigation. *J Neurol Surg A Cent Eur Neurosurg.* 2013;74(2):71-76.

76. Li L, Yang J, Chu Y, Wu W, Xue J, Liang P, Chen L. A Novel Augmented Reality Navigation System for Endoscopic Sinus and Skull Base Surgery: A Feasibility Study *PLoS One.* 2016;11(1):e0146996.

77. Kawamata T, Iseki H, Shibasaki T, Hori T. Endoscopic Augmented Reality Navigation System for Endonasal Transsphenoidal Surgery to Treat Pituitary Tumors: Technical Note. *Neurosurgery.* 2002;50(6):1393-1397.

78. Essig H, Rana M, Meyer A, Eckardt AM, Kokemueller H, Von See C, Lindhorst D, Tavassol F, Ruecker M, Gellrich N-C. Virtual 3D tumor marking-exact intraoperative coordinate mapping improve post-operative radiotherapy. *Rad oncol.* 2011;6(1):159.

79. Wolfgang B. Computer-enhanced stereoscopic vision in a head-mounted operating binocular. *Phys Med Biol.* 2003;48(3):N49-N57.

80. Thoranaghatte R, Garcia J, Caversaccio M, Widmer D, Gonzalez Ballester MA, Nolte LP, Zheng G. Landmark-based augmented reality system for paranasal and transnasal endoscopic surgeries. *Int J Med Robot Comput Assist Surg.* 2009;5(4):415-422.

81. Dixon B, Daly M, Chan H, Vescan A, Witterick I, Irish J. Inattentional blindness increased with augmented reality surgical navigation. *Am J Rhinol Allergy.* 2014;28(5):433-437.

82. Lapeer RJ, Jeffrey SJ, Dao JT, García GG, Chen M, Shickell SM, Rowland RS, Philpott CM. Using a passive coordinate measurement arm for motion tracking of a rigid endoscope for augmented-reality image-guided surgery. *Int J Med Robot.* 2014;10(1):65-77.

83. Zhou Z, Wu B, Duan J, Zhang X, Zhang N, Liang Z. Optical surgical instrument tracking system based on the principle of stereo vision. *J Biomed Opt.* 2017;22(6):065005.

84. Marroquin BR, Lalande BA, Hussain BR, Guigou BC, Grayeli BA. Augmented Reality of the Middle Ear Combining Otoendoscopy and Temporal Bone Computed Tomography. *Otol Neurotol.* 2018;39(8):931-939.

85. Liu WP, Azizian M, Sorger J, Taylor RH, Reilly BK, Cleary K, Preciado D. Cadaveric Feasibility Study of da Vinci Si–Assisted Cochlear Implant With Augmented Visual Navigation for Otologic Surgery. *JAMA Otolaryngol Head Neck Surg.* 2014;140(3):208-214.

86. Chu Y, Yang J, Ma S, Ai D, Li W, Song H, Li L, Chen D, Chen L, Wang Y. Registration and fusion quantification of augmented reality based nasal endoscopic surgery. *Med Image Anal.* 2017;42:241-256.

87. Caversaccio M, Langlotz F, Nolte LP, Häusler R. Impact of a self-developed planning and self-constructed navigation system on skull base surgery: 10 years experience. *Acta Oto-Laryngologica.* 2007;127(4):403-407.

88. Hussain R, Lalande A, Marroquin R, Girum KB, Guigou C, Grayeli AB. Real-Time Augmented Reality for Ear Surgery. *Int Conf Med Image Comput Computer-Assisted Interv.* 2018:324-331.

89. Salb T, Burgert O, Gockel T, Hassfeld S, Muehling J, Dillmann R. Evaluation of INPRES-intraoperative presentation of surgical planning and simulation results. *Stud Health Technol Inform.* 2003;94:309-311.

90. Sudra G, Marmulla R, Salb T, Ghanai S, Eggers G, Giesler B, Hassfeld S, Muehling J, Dillmann R. First clinical tests with the augmented reality system INPRES. *Stud Health Technol Inform.* 2005;111:532-537.

91. Ma L, Jiang W, Zhang B, Qu X, Ning G, Zhang X, Liao H. Augmented reality surgical navigation with accurate CBCT-patient registration for dental implant placement. *Med Biol Eng Comput.* 2019;57(1):47-57.

92. Mischkowski RA, Zinser MJ, Kubler AC, Krug B, Seifert U, Zoller JE. Application of an augmented reality tool for maxillary positioning in orthognathic surgery - A feasibility study. *J Craniomaxillofac Surg.* 2006;34(8):478-483.

93. Espejo Trung LC, Elian SN, Luz MAADC. Development and Application of a New Learning Object for Teaching Operative Dentistry Using Augmented Reality. *J Dent Edu.* 2015;79(11):1356-1362.

94. Liu D, Jenkins SA, Sanderson PM. Clinical Implementation of a Head-Mounted Display of Patient Vital Signs. In. *2009 International Symposium on Wearable Computers* Linz, Austria IEEE; 2009 Sep:47-54.

95. Chang JYC, Tsui LY, Yeung KSK, Yip SWY, Leung GKK. Surgical Vision: Google Glass and Surgery. *Surg Innov.* 2016;23(4):422-426.

96. Simons DJ, Chabris CF. Gorillas in Our Midst: Sustained Inattentional Blindness for Dynamic Events. *Perception.* 1999;28(9):1059-1074.

97. Eckardt BC, Paulo BE. Heads-up Surgery for Vitreoretinal Procedures: An Experimental and Clinical Study. *Retina.* 2016;36(1):137-147.

98. Yoon JW, Chen RE, Kim EJ, Akinduro OO, Kerezoudis P, Han PK, Si P, Freeman WD, Diaz RJ, Komotar RJ, Pirris SM, Brown BL, Bydon M, Wang MY, Wharen RE, Quinones - Hinojosa A. Augmented reality for the surgeon: Systematic review. *Int J Med Robot* 2018;14(4):e1914.

99. Levy LM, Day LJD, Albuquerque LF, Schumaker LG, Giannotta LS, McComb LJG. Heads-up Intraoperative Endoscopic Imaging: A Prospective Evaluation of Techniques and Limitations. *Neurosurgery.* 1997;40(3):526-531.

100. Shibata T, Kim J, Hoffman DM, Banks MS. The zone of comfort: Predicting visual discomfort with stereo displays. *J Vision.* 2011;11(8):11.

101. Muensterer OJ, Lacher M, Zoeller C, Bronstein M, Kübler J. Google Glass in pediatric surgery: An exploratory study. *Int J Surg.* 2014;12(4):281-289.

102. Bosc R, Fitoussi A, Hersant B, Dao TH, Meningaud JP. Intraoperative augmented reality with heads-up displays in maxillofacial surgery: a systematic review of the literature and a classification of relevant technologies. *Int J Oral Maxillofac Surg.* 2019;48(1):132-139.

103. Katić D, Spengler P, Bodenstedt S, Castrillon-Oberndorfer G, Seeberger R, Hoffmann J, Dillmann R, Speidel S. Int J Comput Assist Radiol Surg. *A journal for interdisciplinary research, development and applications of image guided diagnosis and therapy.* 2015;10(1):101-108.

104. van Doormaal TPC, van Doormaal JAM, Mensink T. Clinical Accuracy of Holographic Navigation Using Point-Based Registration on Augmented-Reality Glasses. *Oper Neurosurg* 2019;17(6):588-593.

105. Labadie FR, Davis MB, Fitzpatrick MJ. Image-guided surgery: what is the accuracy? *Curr Op Otolaryngol.* 2005;13(1):27-31.

106. Citardi MJ, Yao W, Luong A. Next-Generation Surgical Navigation Systems in Sinus and Skull Base Surgery. *Otolaryngol Clin North Am.* 2017;50(3):617-632.

107. Yu H, Shen SG, Wang X, Zhang L, Zhang S. The indication and application of computer-assisted navigation in oral and maxillofacial surgery—Shanghai's experience based on 104 cases. *J Cranio Maxillofac Surg.* 2013;41(8):770-774.

108. Wang J, Shen Y, Yang S. A practical marker-less image registration method for augmented reality oral and maxillofacial surgery. *Int J Comput Assist Radiol Surg.* 2019;14(5):763-773.

109. Zhu M, Liu F, Chai G, Pan JJ, Jiang T, Lin L, Xin Y, Zhang Y, Li Q. A novel augmented reality system for displaying inferior alveolar nerve bundles in maxillofacial surgery. *Sci Rep.* 2017;7(1):42365.

110. Zhu M, Chai G, Lin L, Xin Y, Tan A, Bogari M, Zhang Y, Li Q. Effectiveness of a Novel Augmented Reality-Based Navigation System in Treatment of Orbital Hypertelorism. *Ann Plast Surg.* 2016;77(6):662-668.

111. Lin L, Shi Y, Tan A, Bogari M, Zhu M, Xin Y, Xu H, Zhang Y, Xie L, Chai G. Mandibular angle split osteotomy based on a novel augmented reality navigation using specialized robot-assisted arms—A feasibility study. *J Cranio Maxillofac Surg.* 2016;44(2):215-223.

112. Suenaga H, Tran HH, Liao H, Masamune K, Dohi T, Hoshi K, Takato T. Vision-based markerless registration using stereo vision and an augmented reality surgical navigation system: a pilot study. *BMC Med Imaging.* 2015;15:51.

113. Lin GHH, Chang GHW, Wang GCH, Kim GS, Lo GLJ. Three-Dimensional Computer-Assisted Orthognathic Surgery: Experience of 37 Patients. *Ann Plast Surg.* 2015;74 Suppl 2:S118-S126.

114. Junchen W, Suenaga H, Hoshi K, Liangjing Y, Kobayashi E, Sakuma I, Hongen L. Augmented Reality Navigation With Automatic Marker-Free Image Registration Using 3-D Image Overlay for Dental Surgery.

IEEE Trans Biomed Eng. 2014;61(4):1295-1304.

115. Mischkowski RA, Zinser MJ, Kubler AC, Krug B, Seifert U, Zoller JE. Application of an augmented reality tool for maxillary positioning in orthognathic surgery - A feasibility study.(Author abstract). *J Craniomaxillofac Surg.* 2006;34(8):478-483.

116. Tsuji M, Noguchi N, Shigematsu M, Yamashita Y, Ihara K, Shikimori M, Goto M. A new navigation system based on cephalograms and dental casts for oral and maxillofacial surgery. *Int J Oral Maxillofac Surg.* 2006;35(9):828-836.

117. Bettega G, Leitner F. Chirurgie orthognathique assistée par ordinateur : le repositionnement condylien. *Revue de Stomatologie, de Chirurgie Maxillo-faciale et de Chirurgie Orale.* 2013;114(4):205-210.

118. Collyer J. Stereotactic navigation in oral and maxillofacial surgery. *Br J Oral Maxillofac Surg.* 2010;48(2):79-83.

119. Cleary K, Peters TM. Image-guided interventions: technology review and clinical applications. *Biomed Eng.* 2010;12:119-142.

120. Benassarou M, Benassarou A, Meyer C. Computer-assisted navigation in orthognathic surgery. Application to Le Fort I osteotomy. *Rev Stomatol Chir Maxillofac Chir Orale.* 2013;114(4):219-227.

121. Kral F, Puschban EJ, Riechelmann H, Freysinger W. Comparison of optical and electromagnetic tracking for navigated lateral skull base surgery. *Int J Med Robot Comput Assist Surg.* 2013;9(2):247-252.

122. Liu TJ, Ko AT, Tang YB, Lai HS, Chien HF, Hsieh TMH. Clinical application of different surgical navigation systems in complex craniomaxillofacial surgery: the use of multisurface 3-dimensional images and a 2-plane reference system. *Ann Plast Surg.* 2016;76(4):411-419.

123. Wynn W, Frahm C, Carroll P, Clark R, Wellhoner J, Wynn M. Advanced superconducting gradiometer/Magnetometer arrays and a novel signal processing technique. *IEEE Trans Magnet.*

1975;11(2):701-707.

124. Nixon MA, McCallum BC, Fright WR, Price NB. The Effects of Metals and Interfering Fields on Electromagnetic Trackers. *Presence.* 1998;7(2):204-218.

125. Poulin F, Amiot LP. Interference during the use of an electromagnetic tracking system under OR conditions. *J Biomech.* 2002;35(6):733-737.

126. Hummel J, Bax M, Figl M, Kang Y, Maurer C, Birkfellner W, Bergmann H, Shahidi R. Design and application of an assessment protocol for electromagnetic tracking systems. *Med Phys.* 2005;32(7):2371-2379.

127. Kirsch SR, Schilling C, Brunner G. Assesment of metallic distortions of an electromagnetic tracking system. In. *Medical Imaging 2006: Visualization, Image-Guided Procedures, and Display.* Vol 61412006:61410J.

128. Lionberger DR, Weise J, Ho DM, Haddad JL. How Does Electromagnetic Navigation Stack Up Against Infrared Navigation in Minimally Invasive Total Knee Arthroplasties? *J Arthroplasty.* 2008;23(4):573-580.

129. Nafis C, Jensen V, Ron von Jako M. Method for evaluating compatibility of commercial electromagnetic microsensor tracking systems with surgical and imaging tables. In. *Medical Imaging 2008: Visualization Image-Guided Procedures and Modeling.* Vol 6918: International Society for Optics and Photonics; 2008:691820.

130. Thiengwittayaporn S, Junsee D, Tanavalee A. A comparison of blood loss in minimally invasive surgery with and without electromagnetic computer navigation in total knee arthroplasty. *J Med Assoc Thai.* 2009;92(Suppl 6):S27-S32.

131. Tigani D, Busacca M, Moio A, Rimondi E, Del Piccolo N, Sabbioni G. Preliminary experience with electromagnetic navigation system in TKA. *Knee.* 2009;16(1):33-38.

132. Cartellieri FVJKM. Comparison of Six Three-dimensional Navigation Systems During Sinus Surgery. *Acta Oto-Laryngologica.* 2001;121(4):500-504.

133. Cartellieri M, Kremser J, Vorbeck F. Comparison of different 3D navigation systems by a clinical “user”. *Eur Arch Otorhinolaryngol.* 2001;258(1):38-41.

134. Wegner I, Teber D, Hadaschik B, Pahernik S, Hohenfellner M, Meinzer HP, Huber J. Pitfalls of electromagnetic tracking in clinical routine using multiple or adjacent sensors. *Int J Med Robot Comput Assist Surg.* 2013;9(3):268-273.

135. Mucha D, Kosmecki B, Bier J. Plausibility check for error compensation in electromagnetic navigation in endoscopic sinus surgery. *Int J Comput Assist Radiol Surg.* 2006;1:316-318.

136. Berger M, Nova I, Kallus S, Ristow O, Eisenmann U, Freudlsperger C, Seeberger R, Hoffmann J, Dickhaus H. Electromagnetic navigated positioning of the maxilla after Le Fort I osteotomy in preclinical orthognathic surgery cases. *Oral Surg Oral Med Oral Pathol Oral Radiol.* 2017;123(3):298-304.

137. West BJ, Fitzpatrick MJ, Toms AS, Maurer RC, Maciunas JR. Fiducial Point Placement and the Accuracy of Point-based, Rigid Body Registration. *Neurosurgery.* 2001;48(4):810-817.

138. Liu H, Yu Y, Schell MC, O' Dell WG, Ruo R, Okunieff P. Optimal marker placement in photogrammetry patient positioning system. *Med Phys.* 2003;30(2):103-110.

139. Riboldi M, Baroni G, Spadea MF, Tagaste B, Garibaldi C, Cambria R, Orecchia R, Pedotti A. Genetic evolutionary taboo search for optimal marker placement in infrared patient setup. *Phys Med Biol.* 2007;52(19):5815-5830.

140. Atuegwu NC, Galloway RL. Sensitivity analysis of fiducial placement on transorbital target registration error. *International Journal of Computer Assisted Radiology and Surgery.* 2008;2(6):397-404.

141. Wang M, Song Z. Improving target registration accuracy in image-guided neurosurgery by optimizing the distribution of fiducial points. *Int J Med Robot Comput Assist Surg.* 2009;5(1):26-31.

142. Wolfsberger S, Rössler K, Regatschnig R, Ungersböck K. Anatomical landmarks for image registration in frameless stereotactic neuronavigation. *Neurosurg rev.* 2002;25(1-2):68-72.

143. Mascott RC, Sol RJC, Bousquet RP, Lagarrigue RJ, Lazorthes RY, Lauwers-Cances RV. Quantification of True In Vivo (Application) Accuracy in Cranial Image-guided Surgery: Influence of Mode of Patient Registration. *Neurosurgery.* 2006;59(1 Suppl 1):ONS146-156.

144. Metzger MC, Rafii A, Holhweg Majert B, Pham AM, Strong B. Comparison of 4 Registration Strategies for Computer-Aided Maxillofacial Surgery. *Otolaryngol Head Neck Surg.* 2007;137(1):93-99.

145. Grauvogel TD, Soteriou E, Metzger MC, Berlis A, Maier W. Influence of different registration modalities on navigation accuracy in ear, nose, and throat surgery depending on the surgical field. *Laryngoscope.* 2010;120(5):881-888.

146. Makiese O, Pillai P, Salma A, Sammet S, Ammirati M. Accuracy Validation in a Cadaver Model of Cranial Neuronavigation Using a Surface Autoregistration Mask. *Neurosurgery.* 2010;67(3 Operative Neurosurgery 1):ons85-90.

147. Wiles AD, Peters TM. Improved statistical TRE model when using a reference frame. *Med Image Comput Comput Assist Interv.* 2007;10:442-449.

148. Liu W, Ding H, Han H, Xue Q, Sun Z, Wang G. The study of Fiducial Localization Error of image in point-based registration. *Conf Proc IEEE Eng Med Biol Soc.* 2009;2009:5088-5091.

149. Shamir R, Joskowicz L, Spektor S, Shoshan Y. Localization and registration accuracy in image guided neurosurgery: a clinical study. *Int J Comput Assist Radiol Surg.* 2009;4(1):45-52.

150. Shamir RR, Joskowicz L. Geometrical analysis of registration errors in point-based rigid-body registration using invariants. *Med Image Anal.* 2011;15(1):85-95.

151. Balachandran R, Welch EB, Dawant BM, Fitzpatrick JM. Effect of MR Distortion on Targeting for Deep-Brain Stimulation. *IEEE Trans Biomed Eng.* 2010;57(7):1729-1735.

152. Shafiee A, Atala A. Printing Technologies for Medical Applications. *Trends Mol Med.* 2016;22(3):254-265.

153. Bortman J, Mahmood F, Schermerhorn M, Lo R, Swerdlow N, Mahmood F, Matyal R. Use of 3-Dimensional Printing to Create Patient-Specific Abdominal Aortic Aneurysm Models for Preoperative Planning. *J Cardiothorac Vasc Anesth.* 2019;33(5):1442-1446.

154. Rundstedt FC, Scovell JM, Agrawal S, Zaneveld J, Link RE. Utility of patient-specific silicone renal models for planning and rehearsal of complex tumour resections prior to robot-assisted laparoscopic partial nephrectomy. *BJU Int.* 2017;119(4):598-604.

155. Russ M, O'Hara R, Nagesh SS, Mokin M, Jimenez C, Siddiqui A, Bednarek D, Rudin S, Ionita C. Treatment planning for image-guided neuro-vascular interventions using patient-specific 3D printed phantoms. *Proc SPIE Int Soc Opt Eng.* 2015;9417:941726.

156. Midha S, Kumar S, Sharma A, Kaur K, Shi X, Naruphontjirakul P, Jones JR, Ghosh S. Silk fibroin-bioactive glass based advanced biomaterials: towards patient-specific bone grafts. *Biomed Mater.* 2018;13(5):055012.

157. Mavroidis C, Ranky RG, Sivak ML, DiPisa J, Caddle A, Gilhooly K, Govoni L, Sivak S, Lancia M, Drillio R, Patritti BL, Bonato P. Patient Specific Ankle-foot Orthoses Using Rapid Prototyping. *J Neuroeng Rehab.* 2011;8(1).

158. Lin HH, Chang HW, Lo LJ. Development of customized positioning guides using computer-aided design and manufacturing technology for orthognathic surgery. *Int J Comput Assist Radiol Surg.* 2015;10(12):2021-2033.

159. Haefner MF, Giesel FL, Mattke M, Rath D, Wade M, Kuypers J, Preuss A, Kauczor HU, Schenk JP, Debus J, Sterzing F, Unterhinninghofen R. 3D-Printed masks as a new approach for immobilization in radiotherapy - a study of positioning accuracy. *Oncotarget.* 2018;9(5):6490-6498.

160. Yang F, Yao S, Chen KF, Zhu FZ, Xiong ZK, Ji YH, Sun TF, Guo XD. A novel patient-specific three-dimensional-printed external template to guide iliosacral screw insertion: a retrospective study. *BMC musculoskelet disord.* 2018;19(1):397.

161. Gauci MO, Boileau P, Baba M, Chaoui J, Walch G. Patient-specific glenoid guides provide accuracy and reproducibility in total shoulder arthroplasty. *Bone Joint J.* 2016;98-B(8):1080-1085.

162. Hoekstra H, Rosseels W, Sermon A, Nijs S. Corrective limb osteotomy using patient specific 3D-printed guides: A technical note. *Injury.* 2016;47(10):2375-2380.

163. Lin H, Shi L, Wang D. A rapid and intelligent designing technique for patient-specific and 3D-printed orthopedic cast. *3D Print Med.* 2016;2(1):1-10.

164. Lauren M, McIntyre F. A new computer-assisted method for design and fabrication of occlusal splints. *Am J Orthod Dentofacial Orthop.* 2008;133(4):S130-S135.

165. Shaheen E, Sun Y, Jacobs R, Politis C. Three-dimensional printed final occlusal splint for orthognathic surgery: design and validation. *Int J Oral Maxillofac Surg.* 2017;46(1):67-71.

166. Kim BC, Lee CE, Park W, Kim MK, Zhengguo P, Yu HS, Yi CK, Lee SH. Clinical experiences of digital model surgery and the rapid-prototyped wafer for maxillary orthognathic surgery. *Oral Surg Oral Med Oral Pathol Oral Radiol Endod.* 2011;111(3):278-285.

167. Choi JY, Song KG, Baek SH. Virtual model surgery and wafer fabrication for orthognathic surgery. *Int J Oral Maxillofac Surg.* 2009;38(12):1306-1310.

168. Zhang N, Liu S, Hu Z, Hu J, Zhu S, Li Y. Accuracy of virtual surgical planning in two-jaw orthognathic surgery: comparison of planned and actual results. *Oral Surg Oral Med Oral Pathol Oral Radiol.* 2016;122(2):143-151.

169. Zinser MJ, Sailer HF, Ritter L, Braumann B, Maegele M, Zöller JE. A Paradigm Shift in Orthognathic Surgery? A Comparison of Navigation, Computer-Aided Designed/Computer-Aided Manufactured Splints, and "Classic" Intermaxillary Splints to Surgical Transfer of Virtual Orthognathic Planning. *J Oral Maxillofac Surg.* 2013;71(12):2151.e2151-2121.

170. Suojanen J, Leikola J, Stoor P. The use of patient-specific implants in orthognathic surgery: A series of 32 maxillary osteotomy patients. *J Cranio Maxillofac Surg.* 2016;44(12):1913-1916.

171. Dumrongwongsiri S, Lin HH, Niu LS, Lo LJ. Customized Three-Dimensional Printing Spacers for Bone Positioning in Orthognathic Surgery for Correction and Prevention of Facial Asymmetry. *Plast Reconstr Surg.* 2019;144(2):246e-251e.

172. Mazzoni S, Bianchi A, Schiariti G, Badiali G, Marchetti C. Computer-Aided Design and Computer-Aided Manufacturing Cutting Guides and Customized Titanium Plates Are Useful in Upper Maxilla Waferless Repositioning. *J Oral Maxillofac Surg.* 2015;73(4):701-707.

173. Philippe B. Computer designed guides and miniplates in orthognathic surgery: a description of the planning and surgical technique. *Int J Oral Maxillofac Surg.* 2015;44:e123.

174. Brunso J, Franco M, Constantinescu T, Barbier L, Santamaría JA, Alvarez J. Custom-Machined Miniplates and Bone-Supported Guides for Orthognathic Surgery: A New Surgical Procedure. *J Oral Maxillofac Surg.* 2016;74(5):1061.e1061-1061.e1012.

175. Huang SF, Lo LJ, Lin CL. Biomechanical optimization of a custom-made positioning and fixing bone plate for Le Fort I osteotomy by finite element analysis. *Comput Biol Med.* 2016;68:49-56.

176. Mavili EM, Canter IH, Saglam Aydinatay IB, Kamaci IS, Kocadereli II. Use of Three-Dimensional Medical Modeling Methods for Precise Planning of Orthognathic Surgery. *J Craniofac Surg.* 2007;18(4):740-747.

177. Ibrahim D, Broilo TL, Heitz C, de Oliveira MG, de Oliveira HW, Nobre SMW, Dos Santos Filho JHG, Silva DN. Dimensional error of selective laser sintering, three-dimensional printing and PolyJet™ models in the reproduction of mandibular anatomy. *J Craniomaxillofac Surg.* 2009;37(3):167-173.

178. O'neil M, Khambay B, Bowman A, Moos KF, Barbenel J, Walker F, Ayoub A. Validation of a new method for building a three-dimensional physical model of the skull and dentition. *Br J Oral Maxillofac Surg.* 2012;50(1):49-54.

179. Ayoub AF, Rehab M, O'neil M, Khambay B, Ju X, Barbenel J, Naudi K. A novel approach for planning orthognathic surgery: The integration of dental casts into three-dimensional printed mandibular models. *Int J Oral Maxillofac Surg.* 2014;43(4):454-459.

180. Nkenke E, Zachow S, Benz M, Maier T, Veit K, Kramer M, Benz S, Hausler G, Neukam FW, Lell M. Fusion of computed tomography data and optical 3D images of the dentition for streak artefact correction in the simulation of orthognathic surgery. *Dentomaxillofac Radiol.* 2004;33(4):226-232.

181. Uechi J, Okayama M, Shibata T, Muguruma T, Hayashi K, Endo K, Mizoguchi I. A novel method for the 3-dimensional simulation of orthognathic surgery by using a multimodal image-fusion technique.

Am J Orthodon Dentofac Orthoped. 2006;130(6):786-798.

182. Naether S, Buck U, Campana L, Breitbeck R, Thali M. The examination and identification of bite marks in foods using 3D scanning and 3D comparison methods. *Int J Legal Med.* 2012;126(1):89-95.

183. 이군자, 마기중, 임현성. 한국 성인에 적합한 안경테 설계 I: 안경테 전면부 및 다리부 설계를 위한 계측적 연구. *대한시과학회지.* 2000;2(2):61-68.

184. 이관형, 백두진, 고기석. 청년기 한국인 얼굴에 대한 계측적 연구 I. *대한체질인류학회지.* 2000;13(4):345-355.

185. 김인상, 정영준, 이영일. 한국인 코의 Keystone 영역에 대한 해부학 및 방사선학적 분석. *해부· 생물인류학.* 2008;21(1):13-20.

186. Lee W, Park J, Jeong J, Jeon E, Kim H-E, Park S, You H. Analysis of the facial anthropometric data of Korean pilots for oxygen mask design. In. *Proceedings of the Human Factors and Ergonomics Society Annual Meeting.* Vol 56: SAGE Publications Sage CA: Los Angeles, CA; 2012:1927-1931.

187. Kim HJ, Im SW, Jargal G, Lee S, Yi JH, Park JY, Sung J, Cho SI, Kim JY, Kim JI. Heritabilities of facial measurements and their latent factors in Korean families. *Genomics inform.* 2013;11(2):83-92.

188. Ewers R, Schicho K, Undt G, Wanschitz F, Truppe M, Seemann R, Wagner A. Basic research and 12 years of clinical experience in computer-assisted navigation technology: a review. *Int J Oral Maxillofac Surg.* 2005;34(1):1-8.

189. Cevidanes LH, Tucker S, Styner M, Kim H, Chapuis J, Reyes M, Proffit W, Turvey T, Jaskolka M. Three-dimensional surgical simulation. *Am J Orthodon Dentofac orthoped.* 2010;138(3):361-371.

190. Bell RB. Computer planning and intraoperative navigation in orthognathic surgery. *J Oral Maxillofac Surg.* 2011;69(3):592-605.

191. Gateno J, Xia J, Teichgraeber JF, Rosen A. A new technique for the creation of a computerized composite skull model. *J Oral Maxillofac Surg.* 2003;61(2):222-227.

192. Xia JJ, Gateno J, Teichgraeber JF, Christensen AM, Lasky RE, Lemoine JJ, Liebschner MAK. Accuracy of the Computer-Aided Surgical Simulation (CASS) System in the Treatment of Patients With Complex Craniomaxillofacial Deformity: A Pilot Study. *J Oral Maxillofac Surg.* 2007;65(2):248-254.

193. Shirota T, Shiogama S, Watanabe H, Kurihara Y, Yamaguchi T, Maki K, Kamatani T, Kondo S. Three-dimensional virtual planning and intraoperative navigation for two-jaw orthognathic surgery. *J Oral Maxillofac Surg Med Pathol.* 2016;28(6):530-534.

194. Yu HB, Li B, Zhang L, Shen SG, Wang XD. Computer-assisted surgical planning and intraoperative navigation in the treatment of condylar osteochondroma. *Int J Oral Maxillofac Surg.* 2015;44(1):113-118.

195. Bhat S, Shetty S, Shenoy K. Imaging in implantology. *J Indian Prosthodontic Society.* 2005;5(1):10-14.

196. Nelson BJ, Kaliakatsos IK, Abbott JJ. Microrobots for Minimally Invasive Medicine. *Annu Rev Biomed Eng.* 2010;12(1):55-85.

197. Ren H, Kazanzides P. Investigation of attitude tracking using an integrated inertial and magnetic navigation system for hand-held surgical instruments. *IEEE A SME Trans Mechatron.* 2010;17(2):210-217.

198. Birkfellner W, Watzinger F, Wanschitz F, Enislidis G, Kollmann C, Rafolt D, Nowotny R, Ewers R, Bergmann H. Systematic distortions in magnetic position digitizers. *Med Phys.* 1998;25(11):2242-2248.

199. Bucholz RD, Ho H, Rubin JP. affecting the accuracy of stereotactic localization using computerized tomography. *J Neurosurg.* 1993;79(5):667-673.

200. Cartellieri M, Vorbeck F. Endoscopic Sinus Surgery Using Intraoperative Computed Tomography Imaging for Updating a Three-Dimensional Navigation System. *Laryngoscope.* 2000;110(2):292-296.

201. Azarmehr I, Stokbro K, Bell RB, Thygesen T. Surgical Navigation: A Systematic Review of Indications, Treatments, and Outcomes in Oral and Maxillofacial Surgery. *J Oral Maxillofac Surg.* 2017;75(9):1987-2005.

202. Woo SY, Lee SJ, Yoo JY, Han JJ, Hwang SJ, Huh KH, Lee SS, Heo MS, Choi SC, Yi WJ. Autonomous bone reposition around anatomical landmark for robot-assisted orthognathic surgery. *J Cranio Maxillofac Surg.* 2017;45(12):1980-1988.

203. Marchetti C, Bianchi A, Bassi M, Gori R, Lamberti C, Sarti A. Mathematical Modeling and Numerical Simulation in Maxillofacial Virtual Surgery. *J Craniofac Surg.* 2007;18(4):826-832.

204. Tucker S, Cevidanes L, Styner M, Kim H, Reyes M, Proffit W, Turvey T. Comparison of Actual Surgical Outcomes and 3-Dimensional Surgical Simulations. *J Oral Maxillofac Surg.* 2010;68(10):2412-2421.

205. Hsu SSP, Gateno J, Bell RB, Hirsch DL, Markiewicz MR, Teichgraeber JF, Zhou X, Xia JJ. Accuracy of a Computer-Aided Surgical Simulation Protocol for Orthognathic Surgery: A Prospective Multicenter Study. *J Oral Maxillofac Surg.* 2013;71(1):128-142.

국문 초록

전자기적 위치추적을 이용한 악교정 수술을 위한 증강현실 내비게이션 시스템의 정확도 평가

김 성 하

서울대학교 대학원 치의과학과 영상치의학 전공

(지도교수 이 원 진)

1. 목적

악교정 수술에서 중요한 것은 골편을 계획된 위치에 정확하게 위치시키는 것이다. 이를 위해 영상 가이드 수술 시스템의 개발이 이루어졌는데 특히 광학적 추적을 이용한 3D 모델 가이드 수술 시스템이 개선된 수술 결과를 보여왔다. 하지만 카메라와 마커 사이의 송수신이 직결되어야 하는 점과 시각적 마커가 부피가 큰

구조로 구성되어 있다는 단점을 가지고 있는 광학적 추적 시스템과 단조로운 정보만 제공하고 감각적 피드백의 부족으로 현실감이 떨어지는 기존의 3D 모델 가이드 시스템의 한계를 극복하기 위해 우리는 전자기적 위치추적을 이용한 증강현실 악교정 수술 시스템을 개발하였다. 더불어 비침습적인 내비게이션 시스템을 만들기 위해 3D 프린트 기술로 제작된 비침습적 기준 마커도 개발하였다. 그리고 개발된 내비게이션 시스템과 기준 마커에 대한 정확도 평가를 진행하였다.

2. 실험 재료 및 방법

두개골 모형에 스플린트와 정합바디를 연결한 상태로 CT 영상을 획득하였으며 광학적 스캐너를 이용해 해상도가 높은 상악 치열 모델도 얻는다. 이를 이용하여 가상의 두개골 3D 모델을 제작하고 해부학적 구조인 치아 6개를 수술 랜드마크로 추가하여 증강 모델을 제작한다. 이 증강 모델은 지정한 수술 랜드마크들의 좌표를 실시간으로 추적하여 정량화 데이터와 시각화 데이터로 제공하여 술자의 편의성과 수술의 정확도를 높인다.

평판 디스플레이로 제공하는 증강현실 내비게이션 화면은

실시간으로 촬영되는 실제 환자의 영상에 가상의 대상을 겹쳐 보이게 하여 다양한 정보를 술자에게 직관적으로 제공한다. 개발된 증강현실 시스템에서는 기본적으로 실제 환자의 추적 중인 상악 모델 영상과 계획된 위치에 놓여있는 상악 모델 영상, 수술 랜드마크, 골절제선, 교합평면, 상악의 수직축과 두개골 영상이 있다.

정합은 내비게이션 시스템의 정확도에 있어 중요한 부분이다. 간단하게 수행할 수 있으며 적합한 정확도를 가진 정합 방법을 위해 정합바디 복합체 (스플린트, 정합바디, 증강현실 평면 마커)와 3D 깊이 카메라를 사용하였다. 정합 과정은 수술 전에 정합바디 복합체를 이용하여 영상 공간과 실제 환자의 물리적 공간을 연결하는 술전 정합, 수술장에서 수술 직전에 3D 깊이 카메라를 사용하여 카메라 공간과 환자의 물리적 공간을 이어주는 술중 정합으로 이루어진다.

현재 악교정 수술에서는 대부분 기준 마커의 고정방식으로 나사를 이용하여 골편에 직접 고정하는 방식이 사용되고 있으나 우리는 비침습적인 내비게이션 시스템의 개발을 위해 3D 프린트 기술로 제작한 비침습적 기준 마커를 개발하였다. 이 기준 마커는 개발된 정합 방법에 따라 수술장에서 환자에게 부착 후, 정합시

기준점으로 사용하였던 추적 마커로부터의 상대적 위치관계를 기록함으로써 기준점으로 사용하게 되기 때문에 수술과정에서 중첩되는 조작 오차가 없어 정확도를 유지할 수 있다.

개선된 정합 방법과 3D 프린트 기술로 제작한 비침습적 기준 마커의 정확도 평가를 위해 두개골 모형을 이용해 목표정합오차 (TRE, target registration error)를 측정하였다. 실험에 사용된 기준 마커로는 개발한 3D 프린트 기술로 제작한 비침습적 기준 마커와 기존에 많이 사용되던 2가지 방식의 골편 고정 기준 마커 (관골이나 이마에 고정하는 방식)가 사용되었다. 전체적인 시스템의 정합 오차와 각 기준 마커간의 비교를 위해 두개골 모형의 상하악에 10개의 목표 랜드마크를 부착하고 정합 과정을 시행한 후 목표정합오차를 획득하였다.

개발한 증강현실 수술 내비게이션 시스템의 술 중 정확도와 3D 프린트 기술로 제작한 비침습적 기준 마커의 고정성 평가를 위해 x−, y−, z− 방향으로 각각 +3 mm, −3 mm의 직선운동과 롤 (roll), 피치 (pitch), 및 요 (yaw) 방향으로의 회전운동으로 총 9가지의 Le Fort I 악교정 수술을 설계하고 이를 수술계획 수립 소프트웨어로 시뮬레이션한 후 수립 결과를 증강현실 내비게이션

시스템에 적용하였다. 술전과 술중 정합을 진행하고 내비게이션 시스템을 이용하여 계획된 수술을 각 5회씩 수술을 시행한다.

3. 실험결과

실험 결과 개발한 내비게이션 시스템의 목표정합오차는 0.89 ± 0.42 mm로 충분한 정확도를 나타냈다. 또한 3D 프린트 기술로 제작한 비침습적 기준 마커의 목표정합오차도 0.88 ± 0.43 mm로 침습적 골편 고정 기준 마커 (관골에 위치시킨 마커 0.85 ± 0.39 mm, 이마에 위치시킨 마커 0.94 ± 0.44 mm) 와 유사하게 나타났다. Le Fort I 수술 결과는 3D 프린트 기술로 제작한 비침습적 기준 마커가 0.55 ± 0.15 mm로 나타났으며, ANOVA 결과 세 가지 기준 마커 (3D 프린트 기술로 제작한 비침습적 기준 마커, 관골의 골편 고정 기준 마커, 이마의 골편 고정 기준 마커) 간의 통계적인 유의성은 보이지 않았다.

이는 개발된 시스템이 충분한 수술 정확도를 보이며 3D 프린트 기술로 제작한 비침습적 기준 마커 역시 기존에 사용되던 골편 고정 기준 마커 방식과 고정성의 차이가 없어 수술에 적용 가능하다는 것을 보여준다.

4. 결론

이 연구에서는 전자기적 위치추적, 평판 디스플레이, 3D 프린트 기술로 제작한 비침습적 기준 마커를 사용한 증강현실 악교정 수술 내비게이션 시스템을 개발하였다. 이 시스템은 술자가 수술 시 다양한 정보를 제공받아 직관적으로 수술을 시행할 수 있으며 적합한 정확도를 보였고, 환자에게 비침습적인 접근이 가능케 하였다. 이로 인해 악교정수술의 기술과 결과의 향상에 큰 도움이 될 수 있을 것으로 기대된다.

주요어: 증강현실, 내비게이션 시스템, 악교정 수술, 평판 디스플레이, 전자기적 위치추적, 3D 프린트 기술로 제작한 비침습적 기준 마커

학 번: 2013-30630